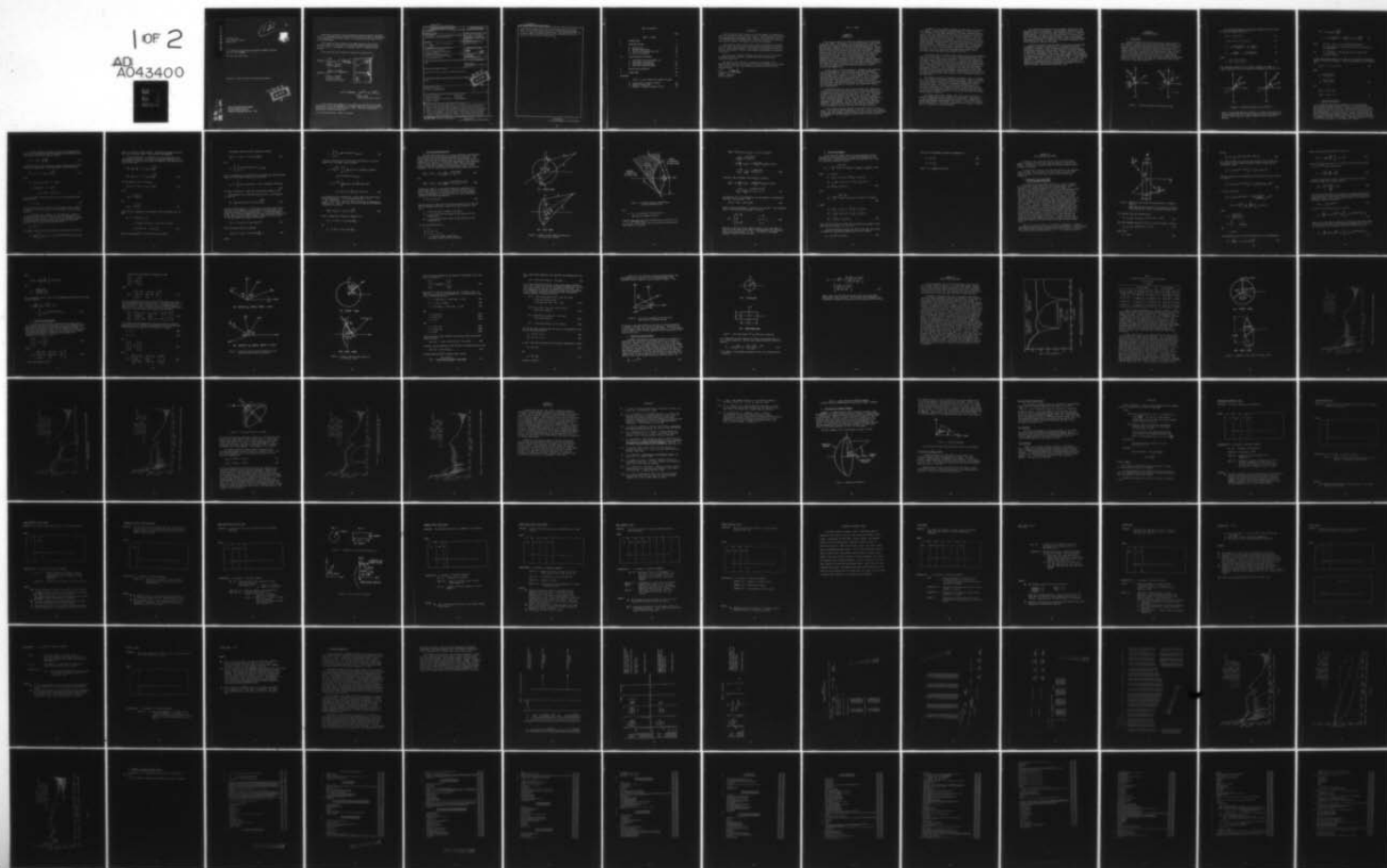


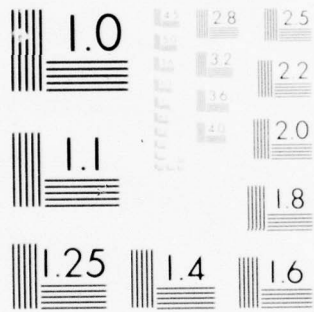
AD-A043 400

OHIO STATE UNIV COLUMBUS DEPT OF ELECTRICAL ENGINEERING F/G 9/1
A GTD ANALYSIS OF THE CIRCULAR REFLECTOR ANTENNA INCLUDING FEED--ETC(U)
AUG 77 S H LEE, R C RUDDUCK, C A KLEIN F30602-76-C-0224
4381-1 RADC-TR-77-259 NL

UNCLASSIFIED

1 of 2
AD
A043400





MICROCOPY RESOLUTION TEST CHART
NATIONAL BUREAU OF STANDARDS-1963-A

ADA043400

12

Q

RADC-TR-77-259
Final Technical Report
August 1977



A GTD ANALYSIS OF THE CIRCULAR REFLECTOR ANTENNA INCLUDING
FEED AND STRUT ANTENNA *scatter*

The Ohio State University ✓

Approved for public release; distribution unlimited.

DDDC
AUG 24 1977
C

AD No.
DDC FILE COPY

ROME AIR DEVELOPMENT CENTER
Air Force Systems Command
Griffiss Air Force Base, New York 13441

This report contains a large percentage of machine-produced copy which is not of the highest printing quality but because of economical consideration, it was determined in the best interest of the government that they be used in this publication.

This report has been reviewed by the RADC Information Office (OI) and is releasable to the National Technical Information Service (NTIS). At NTIS it will be releasable to the general public, including foreign nations.

This report has been reviewed and approved for publication.

APPROVED:

Carmen S. Malagisi

CARMEN S. MALAGISI
Project Engineer

APPROVED:

Joseph L. Ryerson

JOSEPH L. RYERSON
Technical Director
Surveillance Division

ACCESSION for	
NTIS	Write Section <input checked="" type="checkbox"/>
DDC	Buy Section <input type="checkbox"/>
UNANNOUNCED	<input type="checkbox"/>
JUSTIFICATION	
BY	
DISTRIBUTION/AVAILABILITY CODES	
Dist.	id/or SPECIAL
A	

FOR THE COMMANDER:

John P. Huss

JOHN P. HUSS
Acting Chief, Plans Office

If your address has changed or if you wish to be removed from the RADC mailing list, or if the addressee is no longer employed by your organization, please notify RADC (DAP) Griffiss AFB NY 13441. This will assist us in maintaining a current mailing list.

Do not return this copy. Retain or destroy.

UNCLASSIFIED

SECURITY CLASSIFICATION OF THIS PAGE (When Data Entered)

REPORT DOCUMENTATION PAGE		READ INSTRUCTIONS BEFORE COMPLETING FORM
1. REPORT NUMBER RADC-TR-77-259	2. GOVT ACCESSION NO.	3. RECIPIENT'S CATALOG NUMBER
4. TITLE (and Subtitle) A GTD ANALYSIS OF THE CIRCULAR REFLECTOR ANTENNA INCLUDING FEED AND STRUT SCATTER		5. TYPE OF REPORT & PERIOD COVERED Final Technical Report March 1976 - April 1977
7. AUTHOR(s) S. H. Lee, R. G. Kouyoumjian R. C. Rudduck, C. A. Klein		6. PERFORMING ORG. REPORT NUMBER 4381-1
9. PERFORMING ORGANIZATION NAME AND ADDRESS The Ohio State University Electrical Engineering Department Columbus OH 43210		8. CONTRACT OR GRANT NUMBER(s) F30602-76-C-0224
11. CONTROLLING OFFICE NAME AND ADDRESS Rome Air Development Center (OCTS) Griffiss AFB NY 13441		10. PROGRAM ELEMENT, PROJECT, TASK AREA & WORK UNIT NUMBERS 62702F 45060499
14. MONITORING AGENCY NAME & ADDRESS (if different from Controlling Office) Same		12. REPORT DATE August 1977
16. DISTRIBUTION STATEMENT (of this Report) Approved for public release; distribution unlimited.		13. NUMBER OF PAGES 99
17. DISTRIBUTION STATEMENT (of the abstract entered in Block 20, if different from Report) Same		15. SECURITY CLASS. (of this report) UNCLASSIFIED
18. SUPPLEMENTARY NOTES RADC Project Engineer: Carmen S. Malagisi (OCTS)		15a. DECLASSIFICATION/DOWNGRADING SCHEDULE N/A
19. KEY WORDS (Continue on reverse side if necessary and identify by block number) Reflector Antennas Diffraction Numerical Analysis Scattering Geometrical Theory of Diffraction Strut Scattering Computer Program		
ABSTRACT (Continue on reverse side if necessary and identify by block number) Recently, the wide angle side lobes of a circular reflector antenna pattern were calculated by the Geometrical Theory of Diffraction and an overall pattern can be obtained from a combination of GTD and aperture integration methods. In this report, the analysis is extended to include the scattering from the feed supports. The feed support scattering is treated using the concept of equivalent current line source. The cylinder scattering model developed in this report gives the effect of strut scattering on the wide angle side lobes of the reflector. The scattering from the feed struts		

DDC
AUG 24 1977
RESISTIVE
C

406 240

UNCLASSIFIED

SECURITY CLASSIFICATION OF THIS PAGE(When Data Entered)

always has its greatest effect near the scattering cones for each strut. These scattering cones usually give rise to a maximum aperture blockage effect in certain off-principal plane patterns. The analysis given here can be used to compute the complete pattern of any arbitrary plane cut for a practical circular reflector antenna system.



UNCLASSIFIED

SECURITY CLASSIFICATION OF THIS PAGE(When Data Entered)

TABLE OF CONTENTS

	Page
PART I - Theory	
I	INTRODUCTION 1
II	RADIATION PATTERN 4
	A. Primary Feed 4
	B. Aperture-Integration 6
	C. The Two Point Method Using GTD 11
	D. Ring Current Method 15
III	FEED STRUCTURE SCATTERING 17
	A. Equivalent Line Source Model for Feed Support Scattering 17
	B. Coordinate Transformation 21
	C. Feed Horn Scattering Model 27
IV	RESULTS AND DISCUSSIONS 30
V	CONCLUSIONS 40
	REFERENCES 41
PART II - User's Manual for Computer Program	
	A. Description of Computer Program 43
	B. Example Computer Run 66
	C. Appendix - Computer Program Listing 78

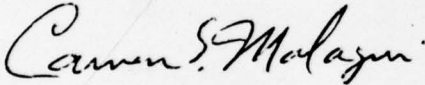
EVALUATION

This contractual effort resulted in the development of a geometrical theory of diffraction (GTD) computer code for circular parabolic reflectors with feed and strut scattering. This computer code analytically predicts the far field pattern of the parabolic reflector including the scattering from reflector edges, feed supports, and the feed structure.

The results of this effort provide a means of simulating a parabolic reflector with obstructing feeds and supporting structures and predicting the far outside lobe responses. This computer code can more accurately simulate the parabolic reflector environment than previously accomplished in the past.

This fits into the RADC Technology Plan (TPO I-B) for analytically simulating parabolic reflector antenna system before fabrication, installation and test.

The computer code, OSU PATT, is presently operational on the RADC-HIS 6180 computer facility and will be used to analyze the performance characteristics of radar and communication parabolic reflector type antenna systems.



CARMEN S. MALAGISI
Project Engineer

PART I - THEORY

CHAPTER I INTRODUCTION

The classical analysis of reflector antennas was well developed in the late 1940's. Accordingly, the radiation pattern in the forward hemisphere of a reflector antenna can be calculated by either the aperture field method or the current distribution method [1]. However, these methods are rather slow for electrically large antennas, and in general do not predict the wide angle side lobes accurately. Recently, the wide angle side lobes were calculated [2] by the GTD [3,4,5] which offers an efficient way to obtain the radiation pattern except for the forward axis region. Thus an overall pattern results from a combination of GTD and aperture integration methods. Using this approach, the far field patterns of the circularly symmetric parabolic reflector antenna with the feed at the focus were calculated in [2]. The effect of a rapid field variation at the edge of the reflector and the coupling between two reflector antennas were also analyzed using the GTD approach [6].

In this report, the same approach is extended to the scattering from the feed supports. Also the analysis has been extended to include calculation of the off-principal plane patterns. The feed horn blockage is also treated in a similar manner to that in [2] by replacing the feed structure by an equivalent circular or rectangular flat plate model whose area approximates the cross section of the feed structure. This approximation is justified in the forward direction, where the feed horn blockage is generally most significant. The flat plate scattering is analyzed by the conventional physical optics approach [7].

On the other hand, the feed support scattering is treated in a different way in which the scattered field of each individual strut is obtained using the concept of equivalent current line source [8,9]. The GTD is used to determine the equivalent line sources. The total effect of the feed support scattering is the sum of the scattered fields from each individual strut. Then the scattering from the feed horn and the feed supports is simply added to the other radiation components of the antenna. Thus the total pattern of the reflector antenna is composed of the radiation field from the reflector, the direct feed pattern and the scattering from the feed structure.

A user-oriented computer program is described in Part II of this report. The input to the program consists of the E- and H-plane patterns of the feed, the frequency, the dimensions of the reflector, the positions and diameters of the feed supports, and the physical cross section of the feed.

In addition to the reflector antenna code described in the body of this report, a second computer code developed by W. D. Burnside and R. F. Marhefka has been made operational on the RADC Honeywell computer system. This code referred to as the flat plate program is used to compute the far-zone scattered fields for antennas radiating in the near zone of structures made of flat plates. In its present form this code simulates structures such as buildings, or ships by a set of finite flat plates forming a convex structure for which the scattering from one flat plate to another is negligible. Using the present code, one can treat the structure by a single flat plate, a rectangular box, a rectangular pyramid, etc. Also a separate ground plane can be introduced. This additional effort was supported by the Naval Ocean Systems Center, San Diego, California under Contract N00123-76-C-1371.

The present code is limited to one structure which can be simulated by as many as 14 plates. This is based on the array dimensions in the code and is not a limitation of the theory. Each plate can consist of 6 corners; however, each corner must lie in a plane or the computer code will abort. The definition of the plates is made by first setting up a fixed cartesian coordinate system relative to the structure under investigation. The plates are, then, defined by the location of the corners. The antenna location is, also, specified in the same coordinate frame. One should note that the fixed coordinate system should be chosen such that one can easily define the structure. The program has the flexibility to handle arbitrary pattern cuts relative to this coordinate system as is discussed later.

The antenna presently considered in the computer code is simulated by a set of electric or magnetic elemental radiators. There is a maximum of six such radiators which is limited by the computer code dimension and not the theory. Each electric or magnetic radiator has cosine distribution, arbitrary length, arbitrary magnitude and phase, and arbitrary orientation. This elemental antenna is considered initially but can be easily modified in that the code is modular in construction. In this case, the SOURCE subroutines can be easily exchanged with another antenna pattern subroutine.

The present form of the computer code is not large in terms of computer storage and executes a pattern in short order. The storage is, of course, dependent on the dimensions which might vary; however, the present code requires approximately 100 K bytes. It will run a pattern cut of 360 points for a flat plate structure with one antenna in approximately 10 seconds on a CDC-6600 computer.

The limitations associated with the computer code results from the basic nature of the analysis. The solution is derived using the Geometrical Theory of Diffraction (GTD) technique which is a high frequency approach. In terms of the scattering from a finite flat plate, this means that each plate should have edges at least a wavelength long. In addition, antenna elements should not get closer than about a wavelength to any edge. In some cases, the previous wavelength limit can be reduced to a quarter wavelength.

A part of the work carried out under this contract concerned the development of diffraction coefficients for perfectly-conducting cylindrical scatterers. These diffraction coefficients were used to calculate the scattering from the feed support of a reflector antenna, as described in the body of this report. However, they also were used to predict the degradation of the pattern of the LAMPS antenna caused by the presence of a nearby cylinder. The LAMPS antenna is a 34" parabolic reflector antenna with a nominal frequency of 4.6 GHz. A report [13] was prepared on this task, and since the results were of interest in the analysis of a shipboard antenna configuration, its publication was supported by NOSC through the Naval Regional Procurement Office, Long Beach, California under Contract N00123-76-C-1371.

CHAPTER II
RADIATION PATTERN

A. Primary Feed

Reflector antennas are classified according to the geometry of the reflector surface as well as the shape of the reflector rim. In this report, a focus-fed paraboloid with circular rim is considered. However, this approach can also be applied to other kinds of reflector antennas. Since the feed is located at the focus, it is convenient to introduce a spherical coordinate system to describe the field of the primary feed with origin at the focus (P_f) and the y axis as the polar axis as shown in Figure 1a. To describe the radiation from the feed at the reflector, another spherical coordinate system also with origin at the focus, but having the z axis as the polar axis is used (see Figure 1b).

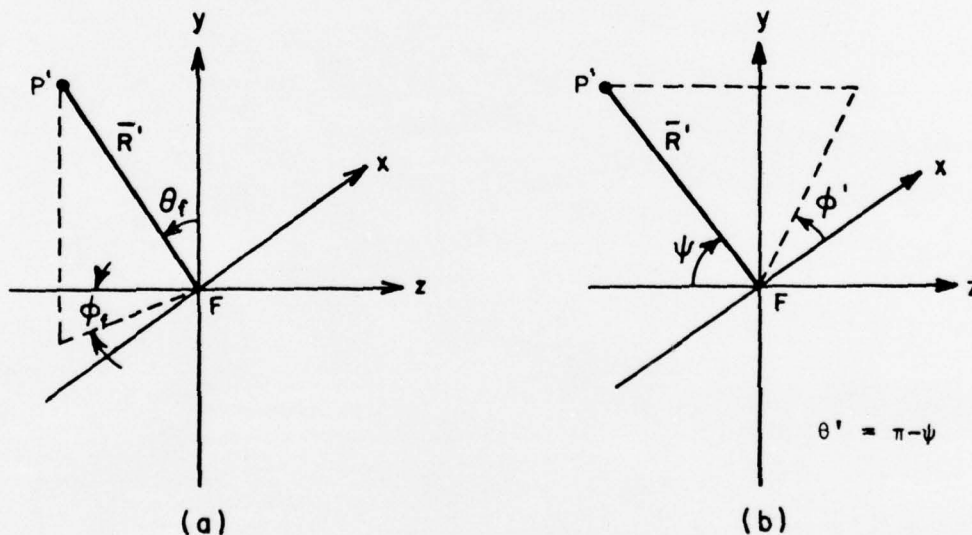


Figure 1. Coordinate systems for the primary feed.

The relations between the coordinate variables and unit vectors of these two systems are given by

$$\cos \psi = \cos \phi_f \sin \theta_f \quad (1)$$

$$-\cos \hat{\phi}' \sin \psi = \sin \phi_f \sin \theta_f \quad (2)$$

$$\hat{\psi} = -\theta_f \frac{\sin \phi' \cos \psi}{B} + \hat{\phi}_f \left(\frac{\cos \phi'}{B} \right) \quad (3)$$

$$\hat{\phi}' = -\hat{\theta}_f \frac{\cos \phi'}{B} - \hat{\phi}_f \frac{\sin \phi' \cos \psi}{B} \quad (4)$$

where

$$B = \sqrt{1 - \sin^2 \psi \sin^2 \phi'} \quad (5)$$

The coordinate systems for the reflector geometry are shown in Figure 2 where (R, θ, ϕ) are the spherical coordinates of the far field

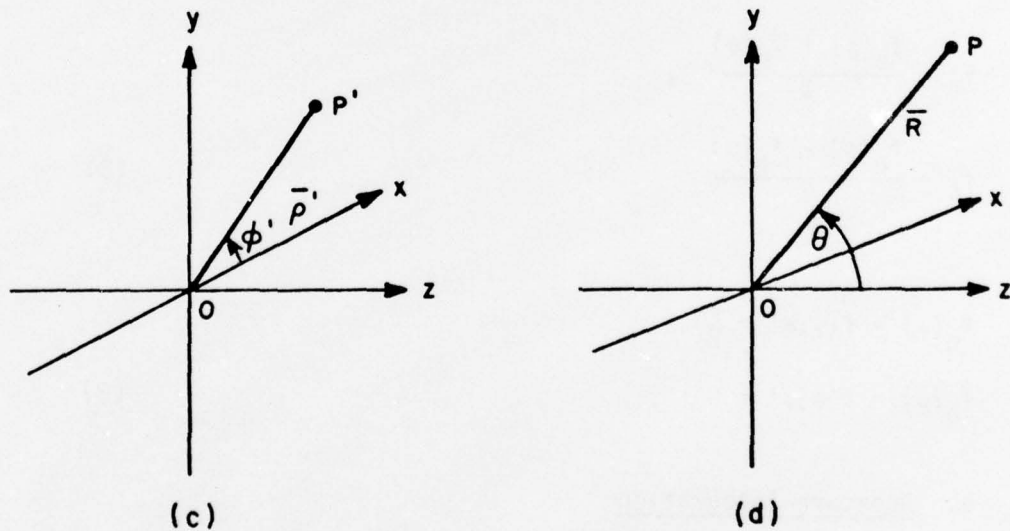


Figure 2. Coordinate systems for the reflector.

point. If we assume that the reflector is in the far zone region of the feed source, the field of the primary feed having the same polarization in the far zone as a dipole oriented in the y direction is given by

$$\begin{aligned} \vec{E}^f &= - \hat{\theta}_f A g(\theta_f, \phi_f) \frac{e^{-jkR'}}{R'} \\ &= - F \left(\hat{\theta} \frac{\cos \psi \sin \phi'}{B} - \hat{\phi} \frac{\cos \phi'}{B} \right) f(\psi, \phi') \frac{e^{-jkR'}}{R'} \end{aligned} \quad (6)$$

where $g(\theta_f, \phi_f) = f(\psi, \phi')$ is the primary feed pattern,
 A is set equal to F , the focal length of the reflection,
for convenience

and $R' = \frac{2F}{1 + \cos \psi}$ is the distance from the feed to the
reflector surface.

In the off-principal planes ($\phi \neq 0, \frac{\pi}{2}$), the feed patterns are approxi-
mated by interpolating between E- and H-plane patterns in the following
way,

$$f(\psi, \phi') = f_T - f_\delta \cos 2\phi' \quad (7)$$

where

$$\begin{aligned} f_T &= \frac{f_e(\psi) + f_h(\psi)}{2} , \\ f_\delta &= \frac{f_e(\psi) - f_h(\psi)}{2} \end{aligned} \quad (8)$$

and

$$\begin{aligned} f_e(\psi) &= f(\psi, \phi' = \frac{\pi}{2}) \\ f_h(\psi) &= f(\psi, \phi' = 0) . \end{aligned} \quad (9)$$

B. Aperture-Integration

In this and the next two sections we are considering the
antenna pattern without aperture blockage or "to calculate most of
the scattering from the reflector". The GTD together with the direct
feed radiation provides a very efficient method to calculate most of
the antenna pattern. The GTD fields can be calculated from only the
feed illumination of the aperture edges. However, the main beam and
the first few sidelobes depend on the fields over the entire aperture.
Consequently, the classical technique of aperture integration is used
to calculate the pattern in the forward axial region.

Using the concepts of geometrical optics and conservation of power, it can be shown [2] that the magnitude of the aperture field is related to that of the incident field by

$$|E^a| = |E^f(R')| \sqrt{R' \frac{d\psi}{d\rho}} \quad (10)$$

It follows from the above expression, adding the appropriate polarization and a phase factor, that the aperture field is given by

$$\vec{E}^a(\rho', \phi') = \hat{e}_r F f(\psi, \phi') \frac{e^{-jkR_0}}{R'} \quad (11)$$

where

$$\begin{aligned} \hat{e}_r &= -\frac{1}{B} [\hat{\rho}' \cos\psi \sin\phi' + \hat{\phi}' \cos\phi'] \\ &= +\frac{1}{B} \left[\frac{1}{2} \sin 2\phi' (1 - \cos\psi) \hat{x} \right. \\ &\quad \left. - (\cos\psi \sin^2\phi' + \cos^2\phi') \hat{y} \right] \quad (12) \end{aligned}$$

R_0 is the distance from the feed to the rim of the reflector (see Figure 4), and

$$\rho' = R' \sin\psi \quad (13)$$

The coordinate system for describing the aperture field is shown in Figure 2a in which the origin is at the center of the reflector aperture.

In evaluating the radiation from the aperture, a spherical coordinate system, shown in Figure 2b, and also centered at 0, is introduced to describe the far zone field of the reflector antenna. By the equivalence principle with image theory, the equivalent magnetic current induced by the aperture field is

$$\vec{K} = 2 \vec{E}^a \times \hat{z} \quad .$$

The pattern function of this equivalent current source is given by

$$\vec{F} = -\frac{jk}{4\pi} \int_0^{2\pi} \int_0^a [\vec{K}(\rho', \phi') \times \hat{r}'] e^{jk\rho' \sin\theta \cos(\phi - \phi')} \rho' d\rho' d\phi' \quad (14)$$

where \hat{r}' is the unit vector along r' , the distance between the field point and the source, and a is the radius of the aperture.

In substituting \bar{E}^a into Equation (14), we consider the x and y polarizations separately. As in [2], the aperture field E_y^a can be approximated by interpolating between the aperture distributions along the principal axes.

$$\begin{aligned}\bar{E}_e^a &= E_y^a(\rho', \frac{\pi}{2}) = -\hat{y} F f_e(\psi) \frac{e^{-jkR_0}}{R'} \\ \bar{E}_h^e &= E_y^a(\rho', 0) = -\hat{y} F f_h(\psi) \frac{e^{-jkR_0}}{R'}\end{aligned}\quad (15)$$

Thus the aperture field is given by

$$E_y^a(\rho', \phi') = T_f(\rho') - \delta_f(\rho') \cos 2\phi' \quad (16)$$

where

$$T_f(\rho') = \frac{E_e^a + E_h^a}{2},$$

and

$$\delta_f(\rho') = \frac{E_e^a - E_h^a}{2} \quad (17)$$

Hence for the y component of the aperture field in Equation (14), we have

$$\begin{aligned}\bar{K}_y \times \hat{r}' &= 2(\hat{y} E_y^a \times \hat{z}) \times \hat{r}' \\ &= 2 \hat{x} E_y^a (\hat{x} \sin\theta \cos\phi + \hat{y} \sin\theta \sin\phi + \hat{z} \cos\theta) \\ &= 2(\hat{z} \sin\theta \sin\phi - \hat{y} \cos\theta) E_y^a\end{aligned}\quad (18)$$

where we have assumed $\hat{r}' \approx \hat{r}$ for far field calculation.

The pattern function of E_y^a is therefore given by

$$\bar{F}_y(\theta, \phi) = (\hat{y} \cos\theta - \hat{z} \sin\theta \sin\phi) \frac{jk}{2\pi} I_y \quad (19)$$

where

$$I_y = \int_0^{2\pi} \int_0^a E_y^a e^{jk\rho' \sin\theta \cos(\phi - \phi')} \rho' d\rho' d\phi' .$$

The ϕ' integration can be analytically evaluated using the well-known properties of the Bessel function J_n ; thus we get

$$I_y = 2\pi \int_0^a [T_f(\rho') J_0(k\rho' \sin\theta) + \delta_f(\rho') \cos 2\phi J_2(k\rho' \sin\theta)] \rho' d\rho' . \quad (20)$$

The above integration is numerically evaluated by Simpson's rule.

Next consider the x polarized aperture field. From Equations (11) and (12)

$$E_x^a = \frac{1}{2B} \sin 2\phi' (1 - \cos\psi) F f(\psi, \phi') \frac{e^{-jkR_0}}{R_1} . \quad (21)$$

In the principal planes ($\phi = 0, \frac{\pi}{2}$), these x polarized fields vanish. Thus only the y-component of the aperture field contributes to the radiation patterns in the principal planes. In the off-principal planes, the x polarized component E_x^a may have significant contribution to the radiation pattern which reaches a maximum in the 45° plane. For the E_x^a component in Equation (14) we have

$$\bar{K}_x \hat{r}' \cong 2(-\hat{x} \cos\theta + \hat{z} \sin\theta \cos\phi) E_x^a . \quad (22)$$

Thus the pattern function F_x becomes

$$\bar{F}_x(\theta, \phi) = (\hat{x} \cos\theta - \hat{z} \sin\theta \cos\phi) \frac{jk}{2\pi} I_x \quad (23)$$

where

$$I_x = \int_0^{2\pi} \int_0^a E_x^a e^{jk\rho' \sin\theta \cos(\phi-\phi')} \rho' d\rho' d\phi' \quad (24)$$

Using the interpolation for the primary feed pattern as given by Equation (8), the above integral becomes

$$\begin{aligned} I_x &= \frac{F e^{-jkR_0}}{2} \int_0^{2\pi} \int_0^a \frac{1}{BR'} [\sin 2\phi' (1-\cos\psi)] [f_T - f_\delta \cos 2\phi'] \\ &\quad \times e^{jk\rho' \sin\theta \cos(\phi-\phi')} \rho' d\rho' d\phi' \\ &= \pi F e^{-jkR_0} \int_0^a \frac{1}{B} [\sin 2\phi (1-\cos\psi) \frac{f_T}{R'} J_2(k\rho' \sin\theta) \\ &\quad + \frac{1}{2} \sin 4\phi (1-\cos\psi) \frac{f_\delta}{R'} J_4(k\rho' \sin\theta)] \rho' d\rho' \quad (25) \end{aligned}$$

In carrying out the ϕ integration, we have made a stationary phase approximation that $\phi' \approx \phi$ in the expression for B, i.e.,

$B = \sqrt{1 - \sin^2\psi \sin^2\phi}$. Again the above integration is evaluated by Simpson's rule. Hence the total far field as obtained from aperture integration is given by

$$\bar{E}(\bar{R}) = [\bar{F}_x(\theta, \phi) + \bar{F}_y(\theta, \phi)] \frac{e^{-jkR}}{R} \quad (26)$$

which is expressed in spherical components by

$$\bar{F}_y = -(\hat{\theta} \sin\phi + \hat{\phi} \cos\theta \cos\phi) \frac{jk}{2\pi} I_y$$

and

$$\bar{F}_x = (\hat{\theta} \cos\phi - \hat{\phi} \cos\theta \sin\phi) \frac{jk}{2\pi} I_x$$

C. Two Point Method Using GTD

The wide angle side lobes of a circular reflector have previously been analyzed by using the two point method based on GTD [2]. This method states that the diffracted field from the paraboloid is contributed mainly by two stationary points, Q_1 and Q_2 on the rim of the reflector (see Figure 3). The detailed formulations of the diffracted field in the E- and H-planes are given in [2]. The off-principal plane diffracted field pattern can be obtained by using a similar procedure. The far zone diffracted fields from Q_1 and Q_2 are given by

$$\vec{E}_1^d(P) = \vec{E}^f(Q_1) \cdot \vec{\bar{D}}(Q_1) \sqrt{\frac{a}{\sin\theta}} \frac{e^{-jk(R-a\sin\theta)}}{R} \quad (27)$$

and

$$\vec{E}_2^d(P) = \vec{E}^f(Q_2) \cdot \vec{\bar{D}}(Q_2) \sqrt{\frac{a}{\sin\theta}} \frac{e^{-jk(R+a\sin\theta) + j\pi/2}}{R} \quad (28)$$

respectively, where $\vec{\bar{D}}$ is the dyadic diffraction coefficient for a curved edge, $E^f(Q_{1,2})$ is the electric field of the feed at $Q_{1,2}$ and a is the radius of the reflector aperture. For rays normally incident on the edge, as is the case here, the dyadic diffraction coefficient [4] can be expressed as:

$$\vec{\bar{D}} = \hat{e} \hat{e} D_s + \hat{p}_d \hat{p}_d D_h \quad (29)$$

where D_s and D_h are the scalar diffraction coefficients for the soft and hard boundary conditions, respectively, and are given in [4], and

\hat{e} is the unit vector tangent to the edge,

$\hat{p} = \hat{e} \times \hat{I}$; \hat{I} being the unit vector in the direction of the incident ray,

$\hat{p}_d = \hat{e} \times \hat{d}$; \hat{d} being the unit vector in the direction of the diffracted ray.

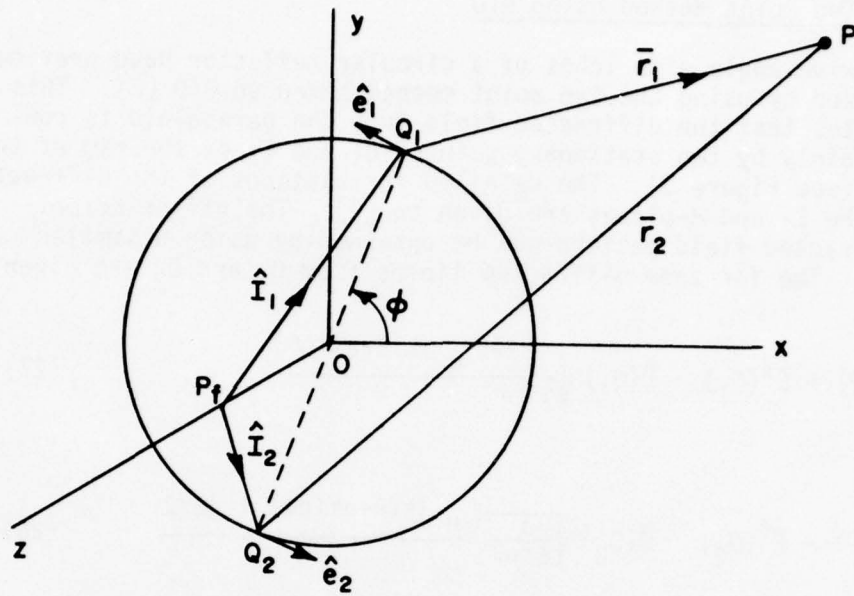
For the ray diffracted at Q_1

$$\hat{e} = \hat{\phi},$$

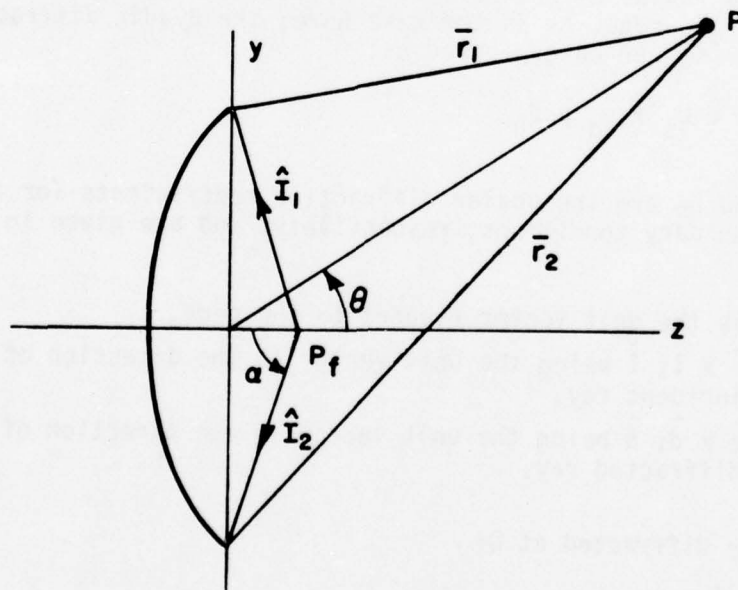
$$\hat{p}_d = \hat{e} \times \hat{d} = \hat{\theta},$$

$$\hat{p} = \hat{e} \times \hat{I}_1 = \hat{\phi} \times \hat{I}_1$$

$\psi = \alpha$ is the half angle spanned from the focus to the rim of the reflector.



(a) FRONT VIEW



(b) SIDE VIEW

Figure 3. Geometry of the edge diffracted rays in an arbitrary ϕ plane.

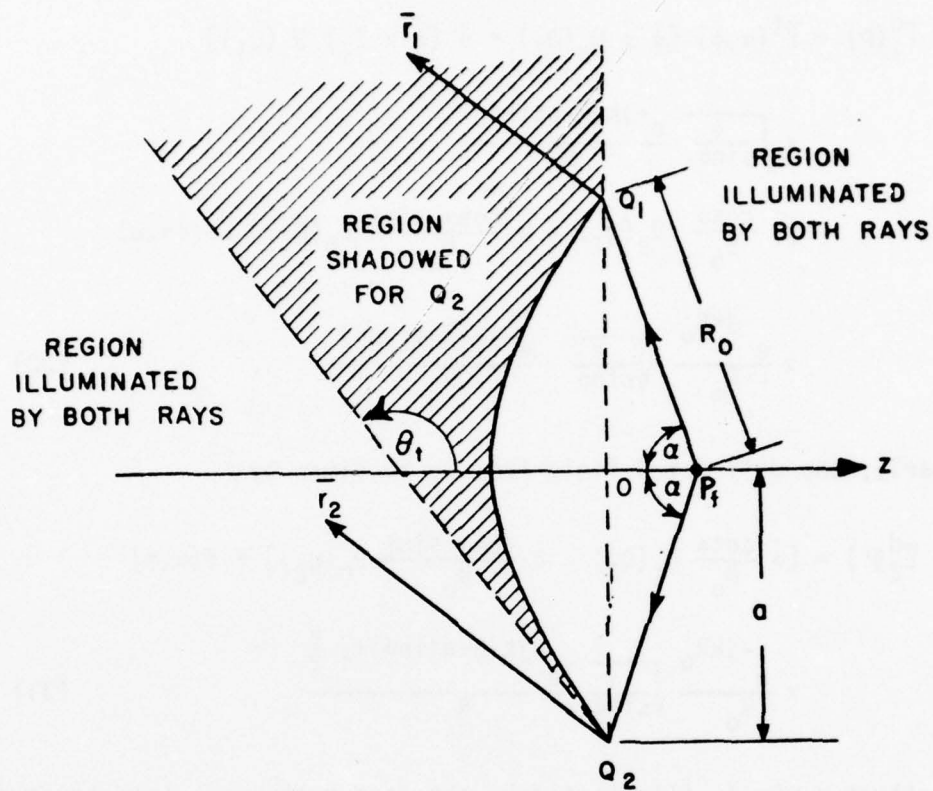


Figure 4. Different regions illuminated by the edge diffracted rays.

and

$R' = R_0$ is the distance from the focus to the rim (see Figures 3 and 4).

Combining Equations (6), (27) and (29) with $\phi' = \phi$ and $\psi = \alpha$ (i.e., $B = B_0 = \sqrt{1 - \sin^2 \alpha \sin^2 \phi}$), the diffracted field from point Q_1 (see Figure 3) is given by

$$\begin{aligned}
\vec{E}_1^d(P) &= \vec{E}^f(\alpha, \phi) [\hat{\phi} \hat{\phi} D_s(Q_1) + \hat{\theta} (\hat{\phi} \times \hat{I}_1) D_h(Q_1)] \\
&\quad \times \sqrt{\frac{a}{\sin\theta}} \frac{e^{-jk(R-a\sin\theta)}}{R} \\
&= [\hat{\phi} \frac{\cos\phi}{B_0} D_s(Q_1) - \hat{\theta} \frac{\cos\alpha \sin\phi}{B_0} D_h(Q_1)] F f(\alpha, \phi) \\
&\quad \times \frac{e^{-jkR_0}}{R_0} \sqrt{\frac{a}{\sin\theta}} \frac{e^{-jk(R-a\sin\theta)}}{R} . \quad (30)
\end{aligned}$$

Similarly, the diffracted field from Q_2 is given by

$$\begin{aligned}
\vec{E}_2^d(P) &= [\hat{\phi} \frac{\cos\phi}{B_0} D_s(Q_2) - \hat{\theta} \frac{\cos\alpha \sin\phi}{B_0} D_h(Q_2)] F f(\alpha, \phi) \\
&\quad \times \frac{e^{-jkR_0}}{R_0} \sqrt{\frac{a}{\sin\theta}} \frac{e^{-jk(R+a\sin\theta)+j\frac{\pi}{2}}}{R} . \quad (31)
\end{aligned}$$

The reflector rim is illuminated by the feed pattern as interpolated from the E- and H-planes. Thus

$$f(\alpha, \phi) = f_T(\alpha) - f_\delta(\alpha) \cos 2\phi \quad (32)$$

where f_T and f_δ are defined in Equations (3a) and (3b). The diffracted field in the different GTD regions is given by

$$\vec{E}^d = \begin{cases} \vec{E}_1^d + \vec{E}_2^d & \theta \leq \frac{\pi}{2} \\ \vec{E}_1^d & \frac{\pi}{2} < \theta < \theta_t \\ \vec{E}_1^d + \vec{E}_2^d & \theta_t \leq \theta \end{cases} \quad (33)$$

where θ_t is the angle of the shadow boundary for Q_2 (see Figure 4). Then the field of the primary feed is superimposed on the diffracted field in the region from $\theta = 0$ to $\theta = \pi - \alpha$ which is the shadow boundary of the field from the feed.

D. Ring Current Method

In the rear axis region, the ring current method is used to calculate the diffracted field, since the two point method is not valid there [2]. The E-plane and H-plane field patterns for θ close to π have been formulated in [2] as

$$\bar{E}_e = -\hat{\theta} \frac{\pi a}{\sqrt{\lambda}} \frac{e^{-j(kR - \frac{\pi}{4})}}{R} [A_1 J_0(x) + A_2 J_2(x) + A_3 J_4(x)], \quad (34)$$

where $x = k a \sin \theta$,

$$\begin{aligned} A_1 &= T_f(D_h - D_s \cos \theta) + \frac{\delta_f}{2} (D_h + D_s \cos \theta), \\ A_2 &= -T_f(D_h + D_s \cos \theta) - \delta_f (D_h - D_s \cos \theta), \\ A_3 &= \frac{\delta_f}{2} (D_h + D_s \cos \theta), \end{aligned} \quad (35)$$

and

$$\bar{E}_h = \hat{y} \frac{\pi a}{\sqrt{\lambda}} \frac{e^{-j(kR - \frac{\pi}{4})}}{R} [B_1 J_0(x) + B_2 J_2(x) + B_3 J_4(x)], \quad (36)$$

where

$$\begin{aligned} B_1 &= T_f(D_s - D_h \cos \theta) - \frac{\delta_f}{2} (D_s + D_h \cos \theta), \\ B_2 &= -T_f(D_s + D_h \cos \theta) + \delta_f (D_s - D_h \cos \theta), \\ B_3 &= -\frac{\delta_f}{2} (D_s + D_h \cos \theta). \end{aligned} \quad (37)$$

Note that the diffraction coefficients D_s and D_h are assumed to have their rear axis values, i.e., for $\theta = \pi$.

In the off-principal planes, the field in the rear axis region is obtained by interpolating between E_e and E_h as follows:

$$E_y = E_e \sin^2 \phi + E_h \cos^2 \phi. \quad (38)$$

This can be transformed to spherical components by

$$E_{\theta} = E_y \sin\phi \quad (39)$$

$$E_{\phi} = E_y \cos\phi \quad (40)$$

since $\pi - \theta$ is assumed to be small.

CHAPTER III FEED STRUCTURE SCATTERING

In practice, the scattering from the feed horn and the feed supports increases the side lobe levels and reduces the gain of the antenna. Therefore, the blocking effect of the feed structure should be taken into account.

To analyze the scattering from the feed structure, two different models are used. An equivalent line source model is used for feed support scattering and a flat plate model is used for feed horn scattering.

A. Equivalent Line Source Model For feed Support Scattering

The effect of the feed support blocking is usually estimated by the projected shadow method in which the feed support or strut is replaced by its effective shadow on the reflector plane. The radiation field from the shadow area is then calculated and subtracted from the antenna pattern [10,11]. In this report, an alternative approach is developed in which the scattered fields from the struts are computed by the equivalent current approach [7]. Since struts often take the form of circular cylinders, only metallic circular cylinder struts are considered here. Also, the incident field on the struts is assumed to be the reflected wave from the reflector only. That is, the interaction of the direct feed radiation and the strut is not considered. The strut scattered field as reflected by the reflector is also neglected. Therefore, the feed support scattering problem is equivalent to a circular cylinder scattering with a plane wave incident at a specified incident angle; however the amplitude of the plane wave can be a slowly-varying function of position. The equivalent current approach is used to take into account the variations of the incident field along each strut, which includes the effect of the finite length of each strut. In this approach, the scattering from each element of a strut is assumed to be the same as that from an element on an infinite cylinder with the same incident field.

Let (x, η, ξ) , (ζ, γ, ξ) and (r, α, γ) denote the rectangular, cylindrical and spherical coordinates of the strut system, respectively. Consider a plane wave incident upon an infinite conducting cylinder of radius a , located at the origin, with an incident angle β , at $\gamma' = \pi$, as shown in Figure 5.

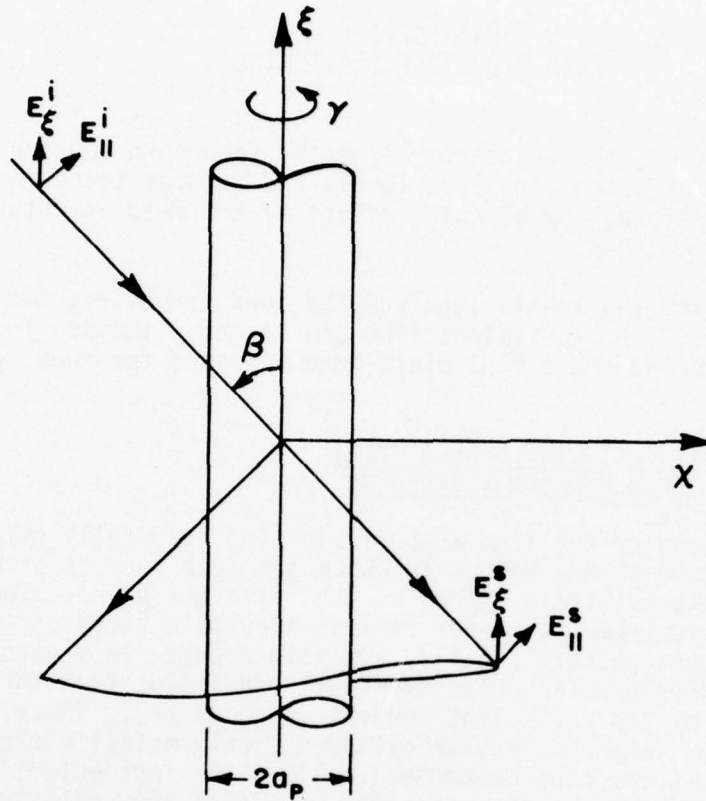


Figure 5. Geometry of the scattering cylinder with an incidence angle β .

(Note that E_ξ and $E_{||}$ both lie in the plane of incidence, which contains the incident ray and the cylinder axis.)

The incident field can be expressed as

$$\vec{E}^i = (\hat{x} \cos\beta + \hat{\xi} \sin\beta) E_0 e^{-jk(x \sin\beta + \xi \cos\beta)} \quad (41)$$

The field component parallel to the axis of the cylinder is given by

$$E_\xi^i = E_{||} \sin\beta e^{-jk(x \sin\beta + \xi \cos\beta)} \quad (42)$$

Noting that

$$x = \xi \cos\gamma \quad (43)$$

we have

$$E_{\xi}^i = E_{\parallel} \sin\beta e^{-jk\xi \cos\beta} e^{-jk\zeta \sin\beta \cos\gamma} . \quad (44)$$

For a wave incident at an angle β with respect to the cylinder axis, the analysis of the cylinder scattering closely follows that for $\beta = 90^\circ$ [7]. Thus

$$E_{\xi}^i = E_{\parallel} \sin\beta e^{-jk\xi \cos\beta} \sum_{-\infty}^{\infty} j^{-n} J_n(k\zeta \sin\beta) e^{-jn\gamma} .$$

Then the scattered field component from the infinite circular cylinder is given by

$$E_{\xi}^S = E_{\parallel} \sin\beta e^{-jk\xi \cos\beta} \sum_{-\infty}^{\infty} j^{-n} a_n H_n^{(2)}(k\zeta \sin\beta) e^{jn\gamma} . \quad (45)$$

In the far field zone

$$\begin{aligned} E_{\xi}^S &\approx E_{\parallel} \sin\beta e^{-jk(\xi \cos\beta + \zeta \sin\beta)} \sqrt{\frac{2j}{\pi k \zeta \sin\beta}} \sum_{-\infty}^{\infty} a_n e^{jn\gamma} \\ &= E_{\parallel} \sin\beta \frac{e^{-jks}}{\sqrt{s}} \frac{1}{\sin\beta} \sqrt{\frac{2j}{\pi k}} \sum_{n=0}^{\infty} \epsilon_n a_n \cos n\gamma \end{aligned}$$

where

$$a_n = - \frac{J_n(ka \sin\beta)}{H_n^{(2)}(ka \sin\beta)}$$

$$\epsilon_n = \begin{cases} 1 & n = 0 \\ 2 & \text{otherwise} \end{cases}$$

and

$$s = \zeta / \sin\beta .$$

The scattered field for parallel polarization can be represented by

$$\bar{E}^S = \hat{\alpha} \frac{E_{\xi}^S}{\sin\beta} = \hat{\alpha} E_{\parallel} D_S(\gamma, \beta) \frac{e^{-jks}}{\sqrt{s}} \quad (46)$$

where the diffraction coefficient is given by

$$D_s(\gamma, \beta) = \frac{1}{\sin \beta} \sqrt{\frac{2j}{\pi k}} \sum_{n=0}^{\infty} \epsilon_n a_n \cos n\gamma \quad (47)$$

Comparing \bar{E}^s with the field of an infinite line source with current $I = I_0 e^{-jk\xi \cos \beta}$, which is given by

$$\bar{E} = -\hat{\alpha} \frac{k^2 I_0}{4\omega\epsilon} \sqrt{\frac{2j}{\pi k}} \frac{e^{-jks}}{\sqrt{s}} \quad (48)$$

we obtain an equivalent electric current line source for the conducting cylinder with a current equal to

$$I_0(\xi) = \frac{4\omega\epsilon}{k^2} \frac{D_s(\gamma, \beta)}{\sqrt{\frac{2j}{\pi k}}} E_{||}(\xi) \quad (49)$$

Then the scattering from a finite section of conducting cylinder can be obtained by calculating the radiation from the equivalent finite length line source. Thus the equivalent current I for the parallel polarized incident field becomes

$$I(\xi) = I_0(\xi) e^{jk\xi \cos \beta} \quad (50)$$

and the far zone radiation field is given by

$$E_{\alpha} = -\sqrt{\frac{jk}{2\pi}} D_s(\gamma, \beta) \frac{e^{-jkr}}{r} \sin \alpha \int_{\xi_1}^{\xi_2} E_{||}(\xi) e^{jk\xi(\cos \alpha + \cos \beta)} d\xi \quad (51)$$

where (r, α, γ) specifies the spherical coordinates of the strut system. Similarly for the electric field component perpendicular to the axis of the cylinder, the scattered field can be obtained from $H_{||}$ as

$$H_{\alpha} = \sqrt{\frac{jk}{2\pi}} D_h(\gamma, \beta) \frac{e^{-jkr}}{r} \sin \alpha \int_{\xi_1}^{\xi_2} H_{||}(\xi) e^{jk\xi(\cos \alpha + \cos \beta)} d\xi \quad (52)$$

where

$$D_h(\gamma, \beta) = \frac{1}{\sin \beta} \sqrt{\frac{2j}{\pi k}} \sum_{n=0}^{\infty} \epsilon_n b_n \cos n\gamma$$

and

$$b_n = - \frac{J'_n(ka \sin \beta)}{H_n^{(2)}(ka \sin \beta)}$$

The corresponding electric field for the perpendicularly polarized incident field is given by

$$E_\gamma = -\sqrt{\frac{jk}{2\pi}} D_h(\gamma, \beta) \frac{e^{-jkr}}{r} \sin \alpha \times \int_{\xi_1}^{\xi_2} E_\perp(\xi) e^{jk\xi(\cos \alpha + \cos \beta)} d\xi \quad (53)$$

B. Coordinate Transformation

In order to add the fields scattered from the feed struts to the radiation field from the reflector, each strut coordinate system needs to be transformed into the reflector coordinate system. As described in the previous section, the rectangular coordinates of the strut coordinate system are denoted by (x, n, ξ) ; and (r, α, γ) denotes the spherical coordinates. The relationship between their respective unit vectors is given by

$$\begin{bmatrix} \hat{r} \\ \hat{\alpha} \\ \hat{\gamma} \end{bmatrix} = [A] \begin{bmatrix} \hat{x} \\ \hat{n} \\ \hat{\xi} \end{bmatrix} \quad (54)$$

where

$$[A] = \begin{bmatrix} \sin \alpha \cos \gamma & \sin \alpha \sin \gamma & \cos \alpha \\ \cos \alpha \cos \gamma & \cos \alpha \sin \gamma & -\sin \alpha \\ -\sin \gamma & \cos \gamma & 0 \end{bmatrix} \quad (55)$$

is the transformation matrix.

Similarly for the reflector coordinate system

$$\begin{bmatrix} \hat{R} \\ \hat{\theta} \\ \hat{\phi} \end{bmatrix} = [B] \begin{bmatrix} \hat{x} \\ \hat{y} \\ \hat{z} \end{bmatrix}$$

where

$$[B] = \begin{bmatrix} \sin\theta \cos\phi & \sin\theta \sin\phi & \cos\theta \\ \cos\theta \cos\phi & \cos\theta \sin\phi & -\sin\theta \\ -\sin\phi & \cos\phi & 0 \end{bmatrix} \quad (57)$$

Now let us transform the (x,y,z) coordinates into the (x,η,ξ) ones. The transformation consists of two steps: first rotate the x axis an angle ϕ_0 about the z axis, then the z axis is rotated an angle θ_0 about the y' (or η) axis, as shown in Figure 6. The resultant transformation can be expressed by the following representation:

$$\begin{bmatrix} \hat{x} \\ \hat{\eta} \\ \hat{\xi} \end{bmatrix} = \begin{bmatrix} \cos\theta_0 \cos\phi_0 & \cos\theta_0 \sin\phi_0 & -\sin\theta_0 \\ -\sin\phi_0 & \cos\phi_0 & 0 \\ \sin\theta_0 \cos\phi_0 & \sin\theta_0 \sin\phi_0 & \cos\theta_0 \end{bmatrix} \begin{bmatrix} \hat{x} \\ \hat{y} \\ \hat{z} \end{bmatrix} \quad (58)$$

If we denote the angle between the strut along the ξ axis and the negative z -axis as β , and the angle between the x -axis and the strut projection on the xy plane as ϕ_s (see Figure 7), we have

$$\phi_0 = \phi_s \quad (59)$$

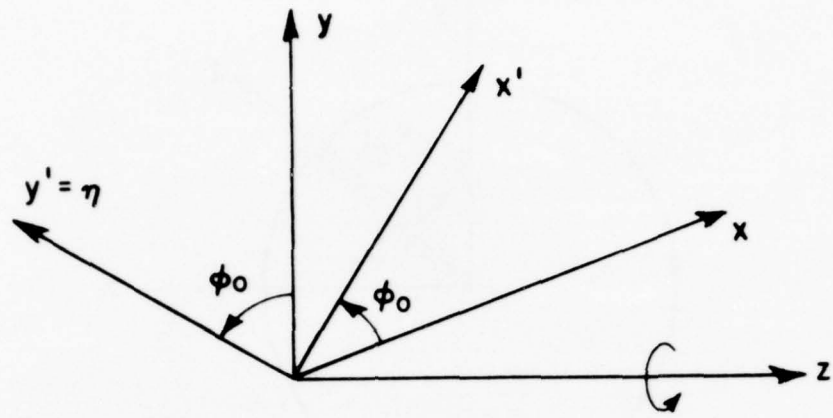
$$\theta_0 = \pi - \beta \quad (60)$$

and

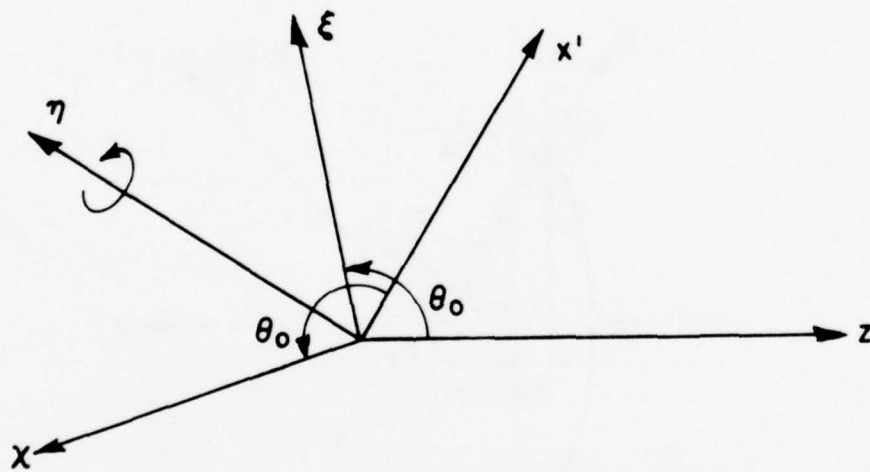
$$\begin{bmatrix} \hat{x} \\ \hat{\eta} \\ \hat{\xi} \end{bmatrix} = [T] \begin{bmatrix} \hat{x} \\ \hat{y} \\ \hat{z} \end{bmatrix} \quad (61)$$

where

$$[T] = \begin{bmatrix} -\cos\beta \cos\phi_s & -\cos\beta \sin\phi_s & -\sin\beta \\ -\sin\phi_s & \cos\phi_s & 0 \\ \sin\beta \cos\phi_s & \sin\beta \sin\phi_s & -\cos\beta \end{bmatrix} \quad (62)$$

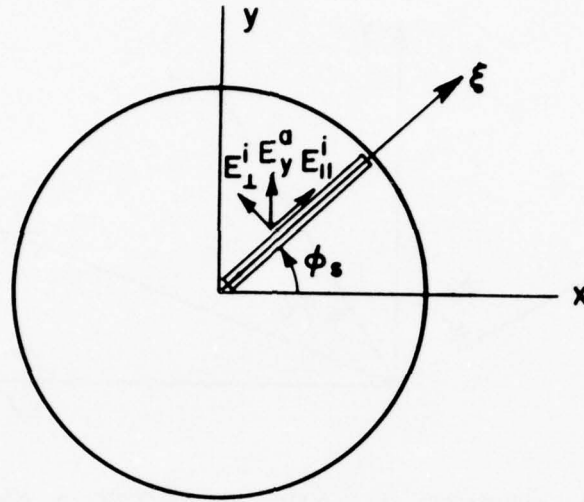


(a) ROTATE ϕ_0 ANGLE ABOUT z AXIS

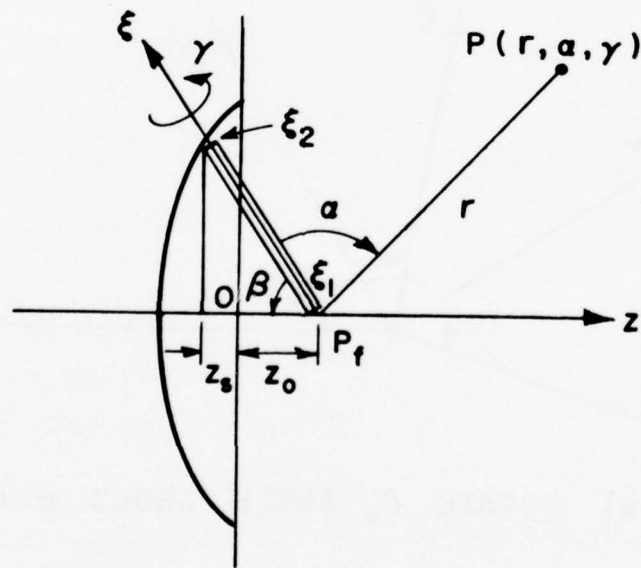


(b) ROTATE θ_0 ANGLE ABOUT η AXIS

Figure 6. Coordinate transformations between the strut and the reflector coordinate systems.



(a) FRONT VIEW



(b) SIDE VIEW

Figure 7. Geometry and coordinate system for an individual strut.

Then the relation between the two spherical coordinates (R, θ, ϕ) and (r, α, γ) is given by

$$\begin{bmatrix} \hat{r} \\ \hat{\alpha} \\ \hat{\gamma} \end{bmatrix} = [A][T][B]^{-1} \begin{bmatrix} \hat{R} \\ \hat{\theta} \\ \hat{\phi} \end{bmatrix} \quad (63)$$

where $[B]^{-1}$ is the inverse matrix of $[B]$. To express α and γ in terms of θ, ϕ, β , and ϕ_S , the components of x, η, ξ are written in the (x, y, z) coordinate system as

$$x = -x \cos\beta \cos\phi_S - y \cos\beta \sin\phi_S - z \sin\beta \quad (64)$$

$$\eta = -x \sin\phi_S + y \cos\phi_S \quad (65)$$

$$\xi = x \sin\beta \cos\phi_S + y \sin\beta \sin\phi_S - z \cos\beta \quad (66)$$

But

$$x = R \sin\alpha \cos\gamma \quad (67a)$$

$$\eta = R \sin\alpha \sin\gamma \quad (67b)$$

$$\xi = R \cos\alpha \quad (67c)$$

and

$$x = R \sin\theta \cos\phi \quad (68a)$$

$$y = R \sin\theta \sin\phi \quad (68b)$$

$$z = R \cos\theta \quad (68c)$$

Putting Equations (67a) and (68) into Equation (64) and combining terms, we obtain

$$\sin\alpha \cos\gamma = - [\sin\theta \cos\beta \cos(\phi - \phi_S) + \cos\theta \sin\beta] \quad (69)$$

Similarly, putting Equations (67b) and (68) into Equation (65), we get

$$\sin\alpha \sin\gamma = \sin\theta \sin(\phi - \phi_S) \quad (70)$$

Dividing Equation (70) by Equation (69), we have

$$\tan \gamma = \frac{\sin\theta \sin(\phi - \phi_S)}{-[\sin\theta \cos\beta \cos(\phi - \phi_S) + \cos\theta \sin\beta]} \quad (71)$$

Also, substituting Equations (67c) and (68) into Equation (66), we get

$$\cos\alpha = \sin\theta \sin\beta \cos(\phi - \phi_S) - \cos\theta \cos\beta \quad . \quad (72)$$

For a given observation direction θ and ϕ , the angular coordinate α and γ for a given strut can be calculated from Equations (71) and (72), where β and ϕ_S specify the orientation of the strut. The field components in the strut coordinate system can be transformed to the reflector coordinate system by using the following dot products obtained from Equation (63) as

$$\begin{aligned} \hat{\alpha} \cdot \hat{\theta} = & -\cos\theta \cos(\phi - \phi_S) [\sin\alpha \sin\beta + \cos\alpha \cos\gamma \cos\beta] \\ & + \cos\alpha \sin\gamma \sin(\phi - \phi_S) \cos\theta \\ & + \sin\theta (\cos\alpha \cos\gamma \sin\beta - \sin\alpha \cos\beta) \end{aligned} \quad (73a)$$

$$\begin{aligned} \hat{\alpha} \cdot \hat{\phi} = & [\sin\alpha \sin\beta + \cos\alpha \cos\gamma \cos\beta] \sin(\phi - \phi_S) \\ & + \cos\alpha \sin\gamma \cos(\phi - \phi_S) \end{aligned} \quad (73b)$$

$$\begin{aligned} \hat{\gamma} \cdot \hat{\theta} = & \sin\gamma [\cos\beta \cos\theta \cos(\phi - \phi_S) - \sin\beta \sin\theta] \\ & + \cos\gamma \cos\theta \sin(\phi - \phi_S) \end{aligned} \quad (73c)$$

$$\hat{\gamma} \cdot \hat{\phi} = -\sin\gamma \cos\beta \sin(\phi - \phi_S) + \cos\gamma \cos(\phi - \phi_S) \quad (73d)$$

Thus the far field scattered from the strut can be expressed in the (R, θ, ϕ) coordinate system as

$$E_{\theta} = \hat{\theta} \cdot \hat{\alpha} E_{\alpha} + \hat{\theta} \cdot \hat{\gamma} E_{\gamma} \quad (74)$$

$$E_{\phi} = \hat{\phi} \cdot \hat{\alpha} E_{\alpha} + \hat{\phi} \cdot \hat{\gamma} E_{\gamma} \quad . \quad (75)$$

E_{α} and E_{γ} are given by Equation (51) and (53), respectively in which

$$E_{\parallel} = E_y^a \sin\phi_S \quad (76)$$

and

$$E_{\perp} = E_y^a \cos\phi_S \quad (77)$$

as shown in Figure 7.

In addition to the coordinate rotation described above, the transformation also consists of a linear displacement of the coordinate centers along the z-axis as shown in Figure 8. Thus

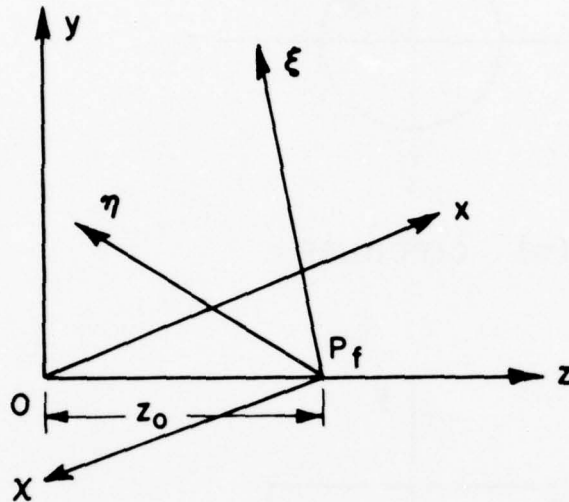


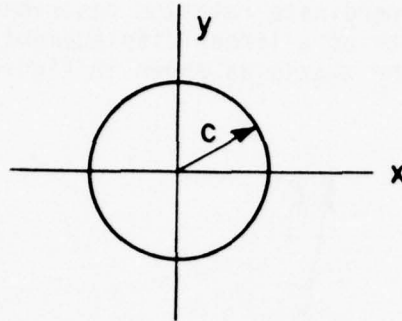
Figure 8. Linear axis placement of the strut and the reflector coordinate systems.

$r=R-z_0\cos\theta$ in the phase expression for the far field approximation in Equations (51) and (53), and $r=R$ in magnitude. The quantity z_0 is the distance between the two coordinate centers, i.e., the distance from the center of the reflector aperture to the intersection of the strut on the z-axis.

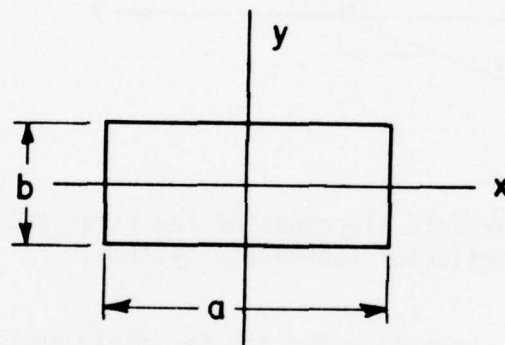
C. Feed Horn Scattering Model

A commonly used method to analyze the feed horn blockage is to assume that the scattering from the feed aperture is the same as that from a conducting flat plate whose area is equal to the cross section of the feed. This approximation is justified in the forward region, where the feed blockage is generally most significant. Then the effect of the aperture radiation being blocked by the feed can be approximated by adding the pattern of the equivalent flat plate to that of the reflector. Since the feed aperture is relatively small compared with the antenna aperture and is located at the center, the aperture field can be assumed uniform over the flat plate. So

$$E_c^a = -\hat{y} e^{-jkR_0} \quad (78)$$



(a) CIRCULAR



(b) RECTANGULAR

Figure 9. Flat plate models for the feed horn scattering.

for a feed with circular aperture of radius C (see Figure 9a), such as a circular feed horn. The far zone scattered field for small θ is given by

$$\vec{E}_c = -\hat{y} \frac{j}{\lambda} \frac{e^{-jkR}}{R} 2\pi c^2 \frac{J_1(k c \sin\theta)}{k c \sin\theta} e^{-jkR_0} \quad (79)$$

If the feed is a rectangular waveguide or horn, the scattered field is given by

$$E_R = -\hat{y} j \frac{e^{-jkR}}{\lambda R} ab \left[\frac{\sin(\frac{\pi a}{\lambda} \sin\theta \cos\phi)}{\frac{\pi a}{\lambda} \sin\theta \cos\phi} \right] \times \left[\frac{\sin(\frac{\pi b}{\lambda} \sin\theta \sin\phi)}{\frac{\pi b}{\lambda} \sin\theta \sin\phi} \right] \quad (80)$$

where a and b are the width and height of the flat plate model, respectively, (see Figure 9b). The scattered field components can be obtained in spherical coordinates by using Equations (39) and (40).

CHAPTER IV RESULTS AND DISCUSSION

Previous analyses [10,11,12] of feed support scattering have usually been limited to angles near the main beam region. However, the cylinder scattering approach developed in this report provides a model to treat the wide angle scattering of each strut. Therefore, in addition to the gain loss, this approach also gives the effect of strut scattering on the wide angle side lobes of the reflector.

According to the geometrical optics assumption, the forward scattering from a cylinder is identical to that from a strip with the same cross section provided that the diameter of the cylinder is large enough. Thus the field obtained from the two solutions should be nearly the same in the forward region. In Figure 10, the scattered pattern of a rectangular strip is compared with that of a vertical circular cylinder ($\beta = 90^\circ$) with uniform incident field, whose E-field is parallel to the cylinder axis. As shown by the curves, the field near the forward axis in the H-plane (transverse to the cylinder axis) agrees within 1 dB for $ka_p = 7$, where a_p is the radius of the strut. For larger ka_p , the difference is even smaller since the geometrical optics approximation of the rectangular strip for the cylinder gets better. For wide angles ($\theta > 20^\circ$), the agreement becomes poorer, because the shadow aperture model is not valid there. Another comparison is made between the Induced Field Ratio (IFR) coefficients in the paper by Rusch et al [12], and those calculated from the equations in this report. The IFR coefficient is defined to be the ratio of the field forward scattered by the cylinder to that of a flat strip with the same physical cross section as the cylinder. Thus the IFR can be obtained from the ratio of Equation (51) with $E_{\parallel} = 1$, $\xi_1 = 0$ and $\xi_2 = L$ to Equation (80) with $a = 2a_p$ and $b = L$. Values of the IFR obtained from this ratio are compared in Table 1 with those calculated by Rusch et al, where the IFR coefficients of [12] are taken from Figure 2 of that paper. The consistency of the two methods in the forward axis region is evident. Since the IFR as defined in [12] is restricted to forward scatter, the results of [12] cannot be used in this work, where the bistatic scattering from the cylindrical strut is required.

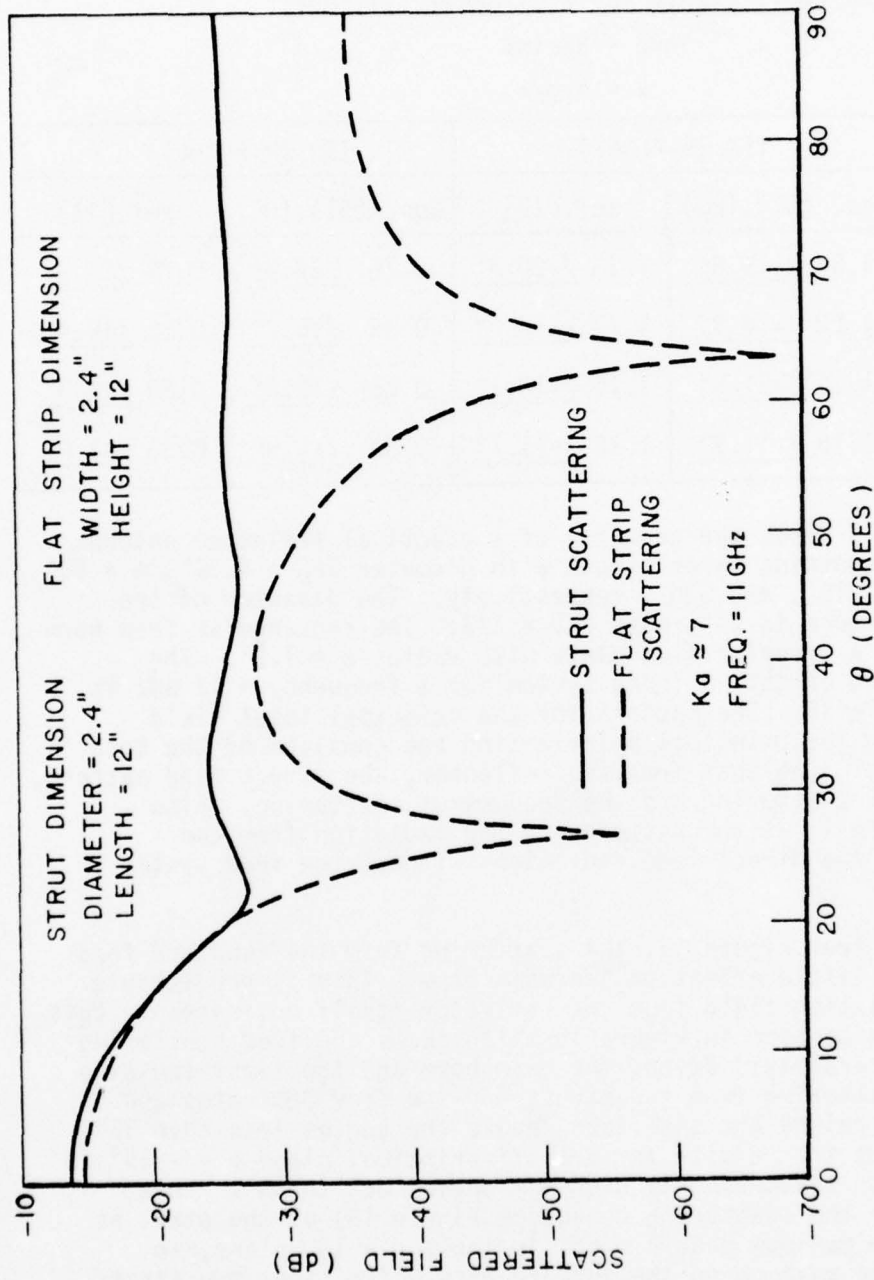


Figure 10. Comparison of the scattering from a circular cylinder (vertical strut) and a flat strip in the H-plane.

Table 1
IFR Coefficients for a Circular Cylinder

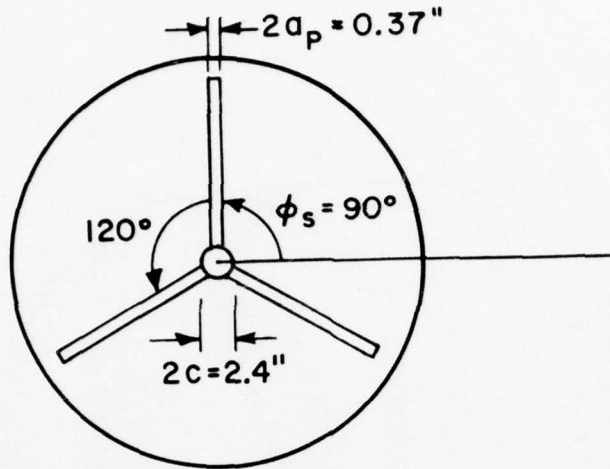
$$\text{Arg} = k a \sin \beta$$

$$x = \text{Arg} / \pi$$

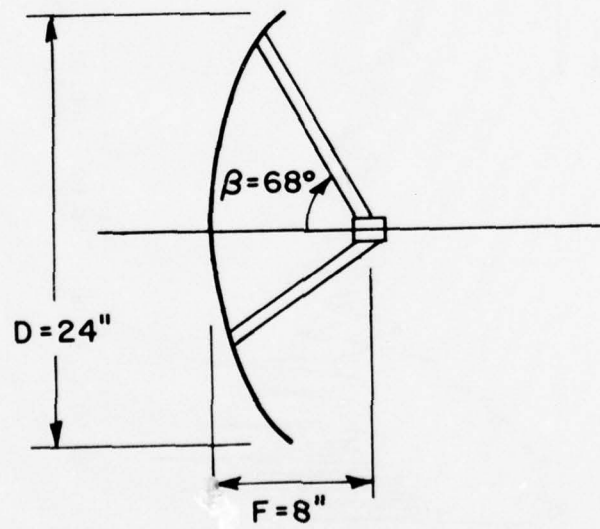
IFR (E-PLANE)				IFR (H-PLANE)	
Arg	x	Eqs. (51),(80)	Ref.[12]	Eqs. (51),(80)	Ref.[12]
2.54	0.81	1.34 <u>/-19.8°</u>	1.33 <u>/-20.3°</u>	0.78 <u>/22.9°</u>	0.79 <u>/21.9°</u>
4.62	1.47	1.22 <u>/-14.3°</u>	1.22 <u>/-15.0°</u>	0.85 <u>/15.7°</u>	0.85 <u>/16.4°</u>
6.74	2.15	1.16 <u>/-11.5°</u>	1.16 <u>/-12.1°</u>	0.88 <u>/12.4°</u>	0.89 <u>/11.5°</u>
7.02	2.24	1.16 <u>/-11.2°</u>	1.15 <u>/-11.7°</u>	0.89 <u>/11.5°</u>	0.90 <u>/11.0°</u>

Figure 11 shows the geometry of a practical reflector antenna system which contains three struts with diameter $2a_p = 0.37"$, $\beta = 68^\circ$ and $\phi_s = 90^\circ, 210^\circ, \text{ and } 330^\circ$, respectively. The diameter of the reflector aperture is $24"$, with $F/D = 1/3$. The rectangular feed horn is mounted in a circular flat plate with radius $c = 1.2"$. The H-plane pattern of this antenna system for a frequency = 11 GHz is shown in Figure 12. The pattern for the principal total field corresponds to the principal polarization and consists of the total radiation, including that from the reflector, the direct feed pattern, the feed model scattering and the feed strut scattering. Also shown in Figure 12 is the pattern for the radiation from the reflector and the direct feed radiation, without the feed system scattering.

As seen from Figure 12, the scattering from the feed and feed struts causes little effect on the main beam. This is predictable since the radiation field from the reflector itself dominates in this region, as can be seen in Figure 13 which shows the feed scattering components separately. Beyond the main beam and the first few side lobes, the scattering from the struts and the feed dominates and substantially raises the side lobe levels for angles less than 35° . Figure 14 shows the results for the off-principal plane $\phi = -15^\circ$ in which the strut scattering is high for angles out to 80° . This occurs because the scattering cone (see Figure 15) of the strut at $\phi_s = 90^\circ$ has a maximum near $\theta = 65^\circ$ in the $\phi = -15^\circ$ plane, in addition to the maximum on the forward axis. The other two struts make less contribution to the scattered field in this plane since their scattering cones are located in different directions. Therefore the feed support scattering effect in the $\phi = -15^\circ$ plane comes mainly from the strut at $\phi_s = 90^\circ$. The scattered field patterns of the



(a) FRONT VIEW



(b) SIDE VIEW

Figure 11. Geometry of the reflector antenna system.

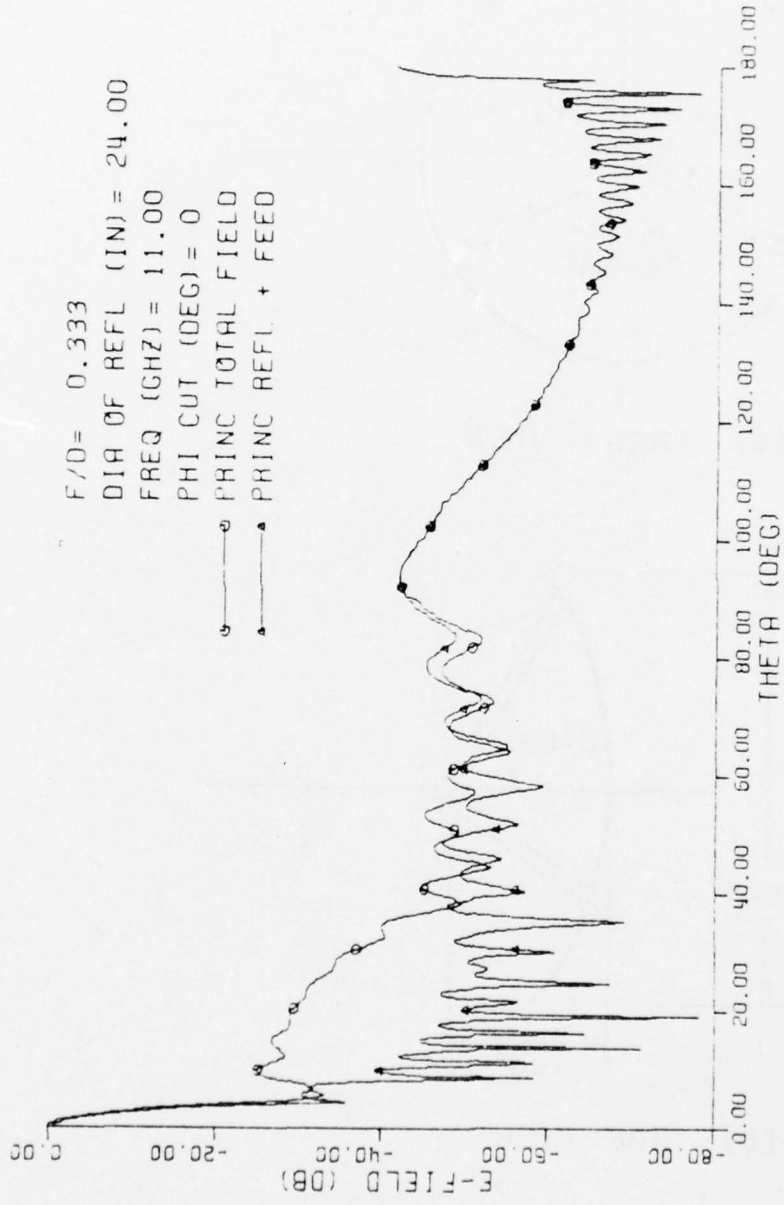


Figure 12. H-plane pattern ($\phi=0$) of the reflector antenna.

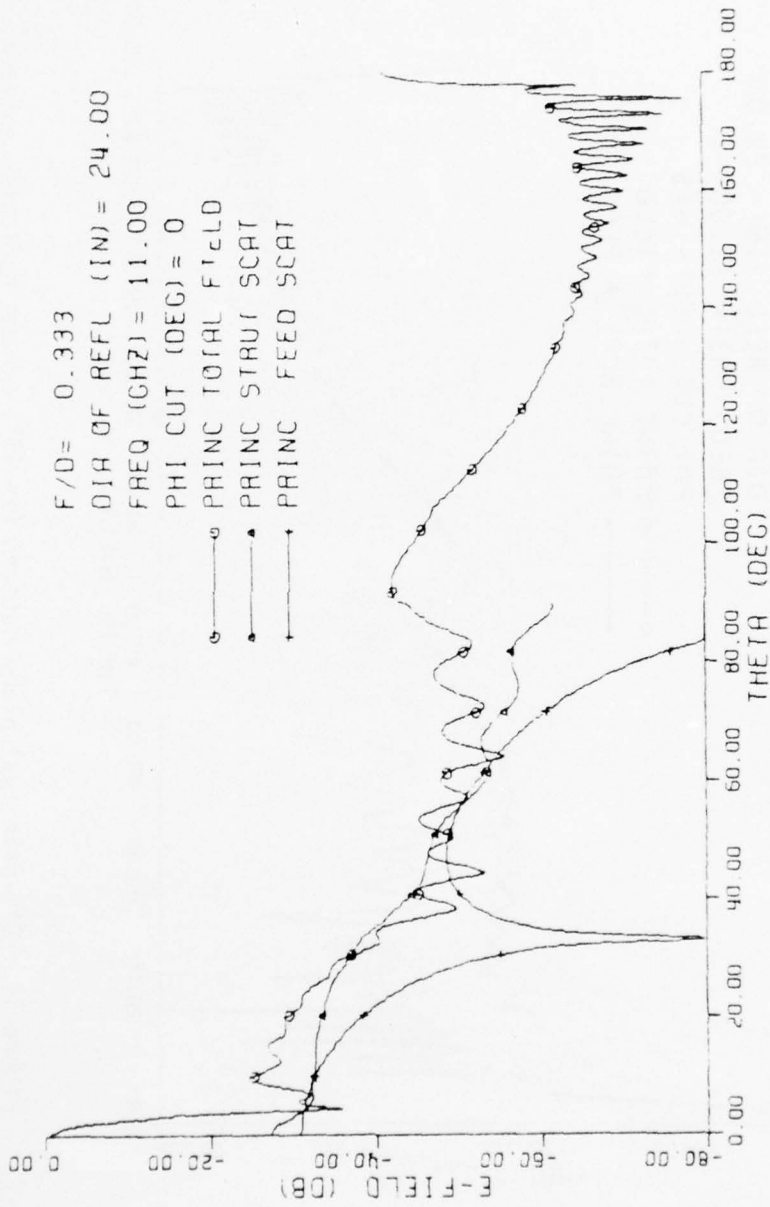


Figure 13. H-plane pattern ($\phi=0$) of the feed strut scattering and feed horn scattering.

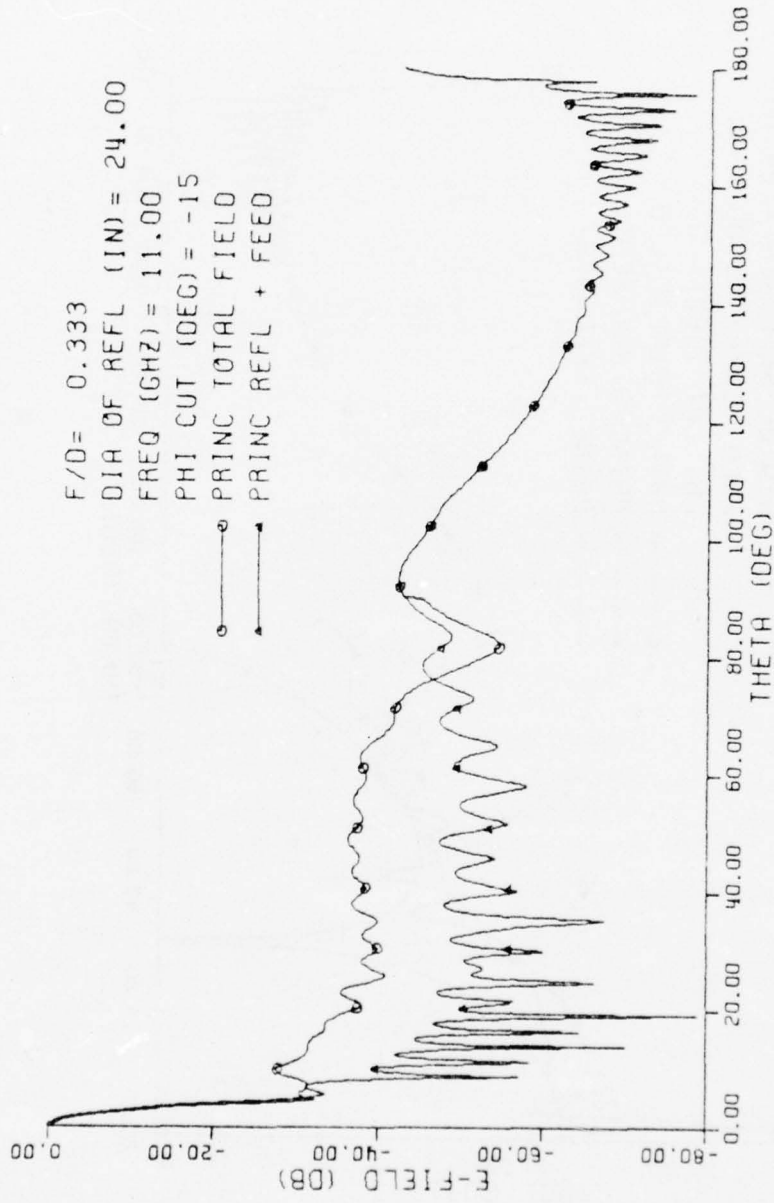


Figure 14. Off-principal plane pattern ($\phi = -15^\circ$) of the reflector antenna.

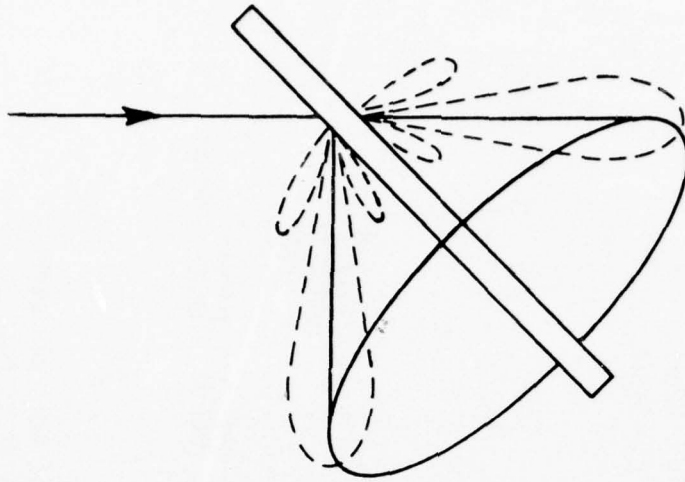


Figure 15. Scattering cone of a cylinder.

struts and the feed horn are shown in Figure 16. Note that the total pattern is no longer symmetric with respect to the z-axis for most off-principal plane cuts as can be seen by comparing Figure 14 and Figure 17 for the $\phi = -15^\circ$ and $\phi = +165^\circ$ plane pattern. Even though the feed pattern (and thus the aperture field) is assumed to be symmetric, the strut geometry is not symmetric in this plane.

The antenna patterns in these figures correspond to the principal polarization, defined in terms of a Huygen's source. Thus the θ and ϕ components can be transformed to principal and cross polarized components by

$$E_{\text{princ}} = \sin\phi E_{\theta} + \cos\phi E_{\phi} \quad (81)$$

$$E_{\text{cross}} = \cos\phi E_{\theta} - \sin\phi E_{\phi} \quad (82)$$

The fields scattered from the feed and struts are shadowed by the reflector surface for much of the rear hemisphere. However, the shadow boundary for the feed support scattering is difficult to define since part of the scattered field is blocked by the reflector as θ approaches 90° , and this blocking keeps on increasing as θ passes 90° until the scattered field is totally blocked out at $\theta = \pi - \alpha$, the shadow boundary for direct feed radiation. For simplicity, the shadow boundary for the feed support and feed horn scattering is set at $\theta = 90^\circ$. This approximation should be reasonable since the scattered field from the struts is usually small at pattern angles $\theta > 90^\circ$. However, a slight discontinuity still exists in the pattern at $\theta = 90^\circ$ because of this truncation.

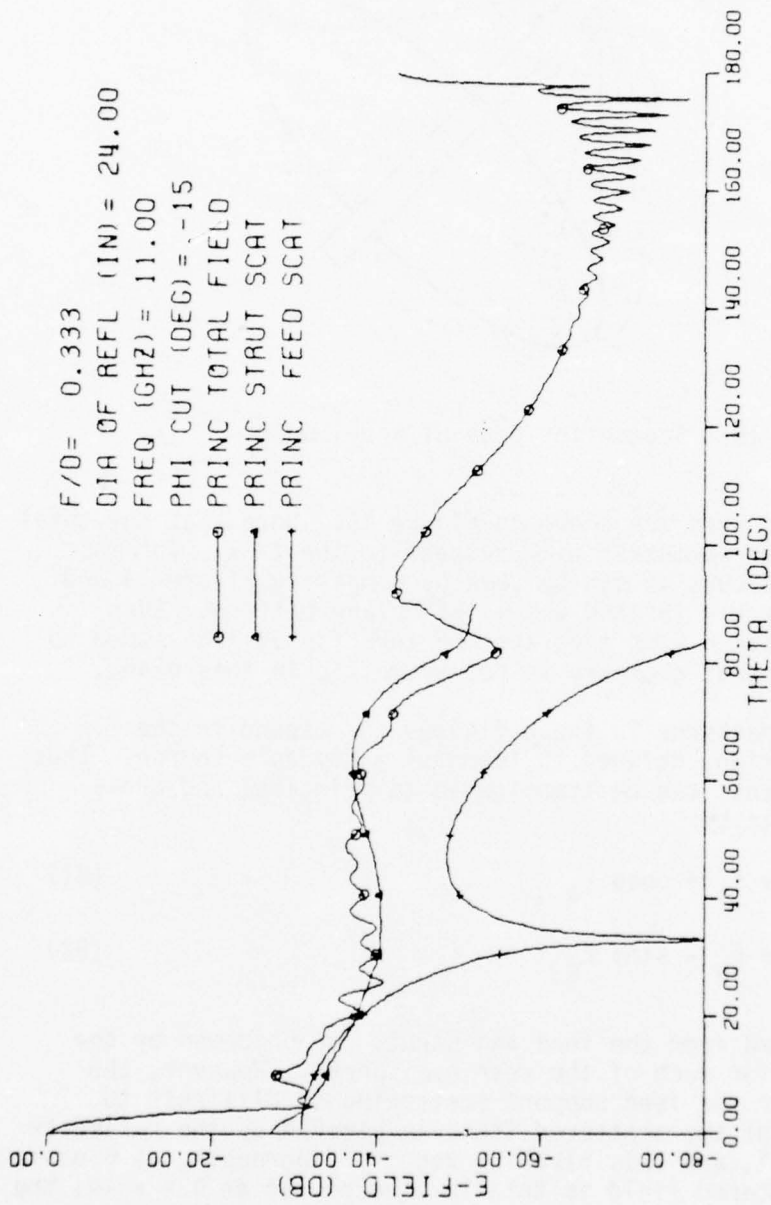


Figure 16. Off-principal plane ($\phi = -15^\circ$) of the feed strut scattering and the feed horn scattering.

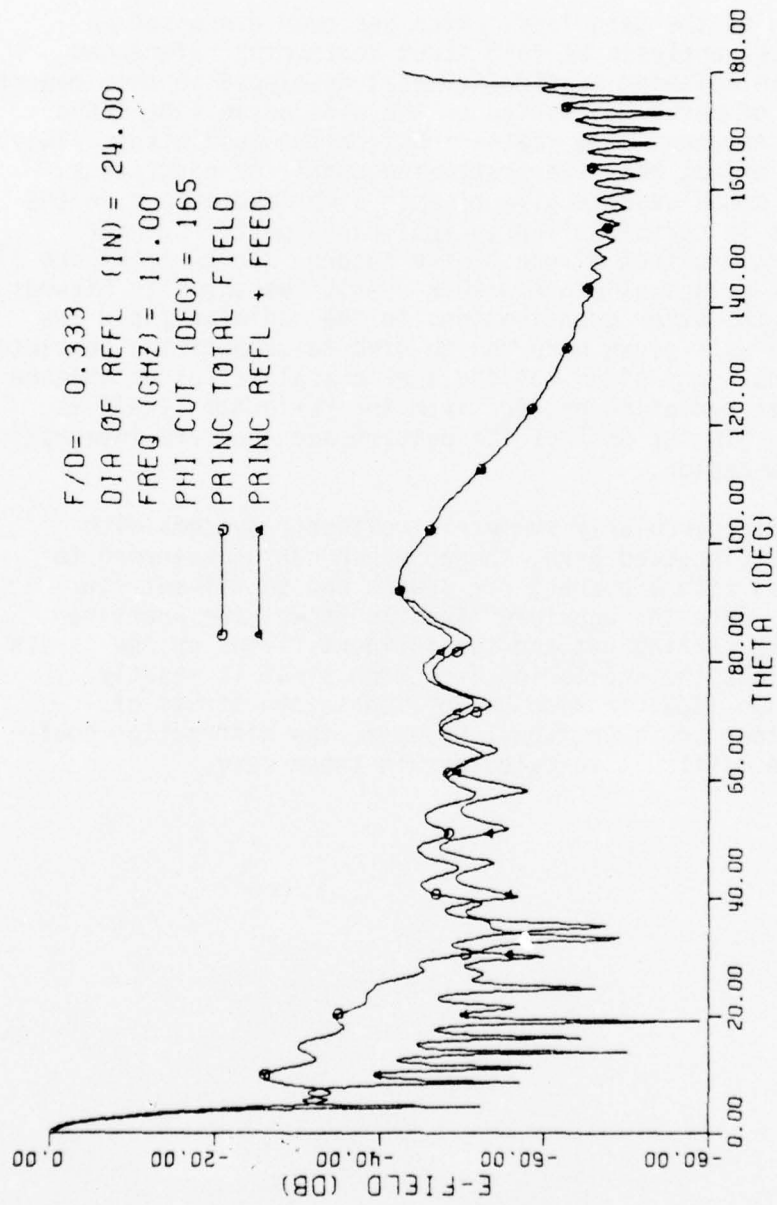


Figure 17. Off-principal plane pattern ($\phi=+165^\circ$) of the reflector antenna.

CHAPTER V CONCLUSIONS

In addition to the gain loss, which has been discussed in previously reported analyses of feed strut scattering referenced in Chapter IV, the cylinder scattering model developed in this report gives the effect of strut scattering on the wide angle side lobes of the reflector antenna. The scattering from the feed struts always has its greatest effect near the scattering cones for each strut. These scattering cones usually give rise to a maximum effect on the antenna sidelobes in certain off-principal plane patterns. For example, the maximum effect of one of the antenna struts in Figure 11 occurs in the off-principal plane with $\phi = -15^\circ$ as shown in Figures 14 and 16. When the other contributions to the radiated field are included, the analysis given here can be used to compute the complete pattern of any arbitrary plane cut for a practical reflector antenna system. The basic radiation pattern from the reflector itself is obtained by using GTD for most of the pattern and aperture integration for the main beam region.

Although only circularly symmetric reflector systems with focused feeds are discussed here, the approach can be extended to reflector antennas with arbitrary rim shapes and to off-set fed systems as well. Once the aperture field is known, the aperture integration can be carried out and the incident fields on the struts are available. Thus the scattering from each strut is readily obtained. The same idea can also be applied to the struts of rectangular or other cross sections; however, the diffraction coefficients are more difficult to calculate in these cases.

REFERENCES

- [1] S. Silver, "Microwave Antenna Theory and Design," MIT Rad. Lab. Series, Vol. 12, McGraw-Hill, 1949.
- [2] R. A. J. Ratnasiri, R. G. Kouyoumjian, and P. H. Pathak, "The Wide Angle Sidelobes of Reflector Antennas," Report 2183-1, 23 March 1970, The Ohio State University ElectroScience Laboratory, Department of Electrical Engineering; prepared under Contract AF 19(628)-5929 for Air Force Cambridge Research Laboratories. (AFCRL-69-0413) (AD 707 105).
- [3] J. B. Keller, "Geometrical Theory of Diffraction," Journal of the Optical Society of America, 52, February 1962, pp. 116-130.
- [4] R. G. Kouyoumjian and P. H. Pathak, "A Uniform Geometrical Theory of Diffraction for an Edge in a Perfectly Conducting Surface," Proc. IEEE, 62, November 1974, pp. 1448-1461.
- [5] R. G. Kouyoumjian, "The Geometrical Theory of Diffraction and Its Application," Topics in Applied Physics, Vol. 3: Numerical and Asymptotic Techniques in Electromagnetics, Edited by R. Mittra, Springer-Verlag, Berlin, Heidelberg, New York, 1975.
- [6] T. Tuvinun, "Application of the GTD to the Analysis of Reflector Antennas," M.Sc. Thesis, The Ohio State University, Columbus, Ohio, 1975.
- [7] R. F. Harrington, Time-Harmonic Electromagnetic Fields, The McGraw-Hill Co., 1961, p. 116.
- [8] C. E. Ryan, Jr. and R. C. Rudduck, "Radiation Patterns of Rectangular Waveguides," IEEE Trans. Antennas and Propagation Comm., AP-16, July 1968, pp. 488-489.
- [9] G. L. James and V. Kerdemelidis, "Reflector Antenna Radiation Pattern Analysis by Equivalent Edge Currents," IEEE Trans., Vol. AP-21, No. 1, January 1973, pp. 19-24.
- [10] C. L. Gray, "Estimating the Effect of Feed Support Member Blocking on Antenna Gain and Side Lobe Level," Microwave Journal, Vol. 7, No. 3, March 1964, pp. 88-91.

- [11] J. Ruze, "Feed Support Blockage Loss in Parabolic Antennas,"
Microwave Journal, Vol. 11, No. 12, 1968, pp. 76-80.
- [12] W. V. T. Rusch et al, "Forward Scattering from Square Cylinders
in the Resonance Region with Application to Aperture Blockage,"
IEEE Trans., Vol. AP-24, No. 2, March 1976, pp. 182-189.
- [13] R. G. Kouyoumjian, R. J. Luebbers, and R. C. Rudduck,
"A GTD Analysis of the LAMPS Antenna Blocked by a Mast,"
Report 4508-3, The Ohio State University ElectroScience Laboratory,
Department of Electrical Engineering; prepared under Contract
N00123-76-C-1371 for Naval Regional Procurement Office, Long
Beach, California 90822. 31 March 1977.

PART II - USER'S MANUAL FOR COMPUTER PROGRAM
"CIRCULAR REFLECTOR ANTENNA WITH FEED AND STRUT SCATTER" (OSUPATT)

A. Description of Computer Program

OSUPATT is a computer program which calculates the total field radiated by a circularly symmetric parabolic reflector including effects of scattering by a number of circularly cylindrical struts and blockage by the feed horn. The user is free to specify the geometry of the reflector, the size of the feed horn cross-section, both the E- and H-planes of the feed pattern, and the size and orientation of the struts. This brief user's document will indicate the methods used and the limitations of the program, and required formats for input data; details of the theory are given in Part I of this report.

The basic geometry used in the program is shown in Figure 1.

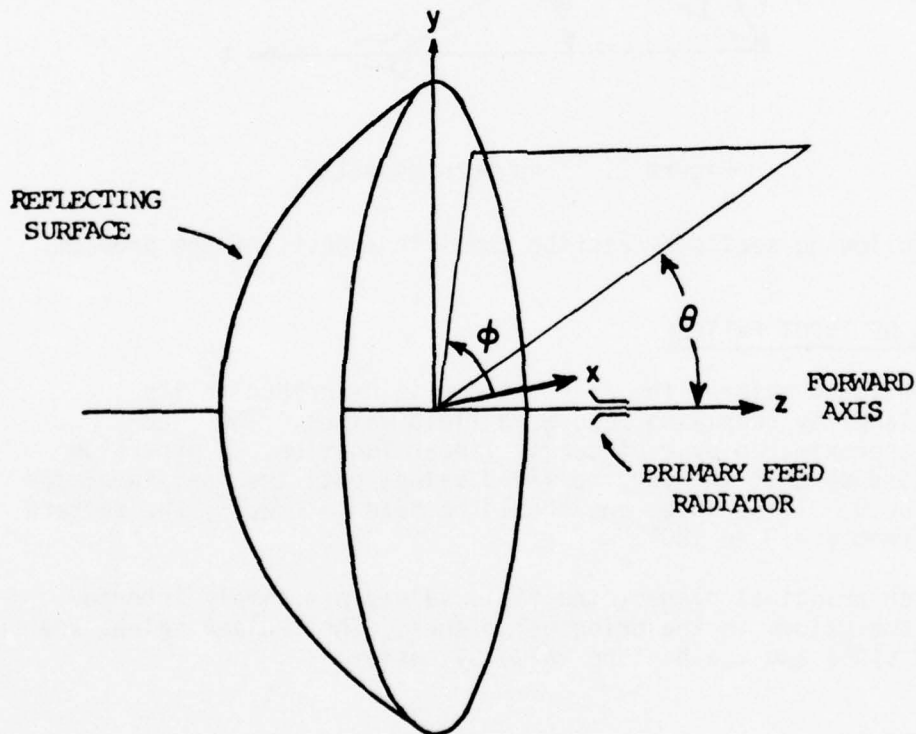


Figure 1. Geometry of Reflector.

The reflector points in the +z direction with the feed located at the focus of the parabola. The polarization of the feed is linear in the +y direction; thus E_ϕ is the principal polarization in the $\phi = 0$ plane and E_θ is the principal polarization in the $\phi = 90^\circ$ plane. The E-plane of the feed horn and the reflector is thus the yz plane and the H-plane is the xz plane. The struts must be oriented so that each strut projects through the z axis. At this time the principal plane feed patterns must be symmetric. These patterns are specified by listing field values for discrete values of ψ , the angle away from the -z axis (see Figure 2).

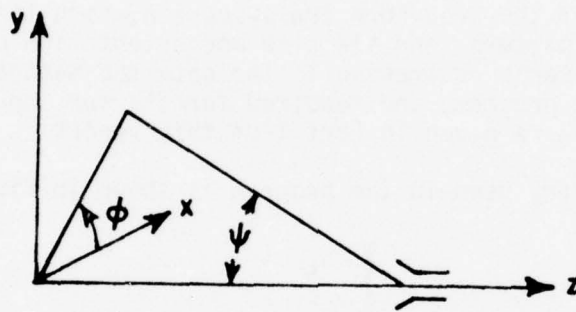


Figure 2. Feed horn geometry.

The following sections describe specific aspects of the problem.

DESCRIPTION OF INPUT PATTERN

As mentioned before, the feed pattern is described in its principal planes by supplying tabulated field values. The feed pattern is approximated by a piecewise linear function. A provision has been added so that the assumed field values past the last tabulated value will be 0. To be safe, one should be sure to specify the pattern explicitly from $\psi = 0$ to 180° .

Between principal planes, the field values are simply interpolated from the values in the principal planes. The E-plane values are weighted by $\sin^2\phi$ and the H-plane value by $\cos^2\phi$.

REFLECTOR PATTERN CALCULATION

The reflector's secondary pattern is calculated by two different methods over two different ranges of polar angle θ . For small θ ($\frac{kD}{2} \sin \theta < 24$), the aperture fields are integrated as specified by physical optics. Due to the symmetry of this problem, the integration is still one dimensional and thus relatively large apertures can be used without prohibitive computer costs. For θ angles past the limit, the Geometrical Theory of Diffraction (GTD) is used. The fields calculated by the program are all normalized by the peak field of the reflector by itself. Any direct field from the feed is also included in the total field.

FEED BLOCKAGE

The effect of blockage by a feed cross-section is very simply modeled in the forward direction by Kirchhoff's method. When a rectangular feed is specified, the scattered pattern has the familiar $\sin(x)/x$ shaped pattern in each principal direction while for a circular feed, the pattern has $J_1(x)/x$ variation.

STRUT BLOCKAGE

Scattering by circular cylindrical struts is calculated by first finding the equivalent currents on segments of the struts and then integrating the reradiated fields which are produced by these currents. The equivalent currents are calculated from the diffraction coefficients of the cylindrical strut cross-section and the incident aperture field. The diffraction coefficients are a summation of eigenmodes for the circular cylinder.

LIMITATIONS

Due to limitations in theory or the arrangement of the computer program, the following limits should be observed.

STRUTS

STRUT must not extend past z axis, i.e., RL02 must not exceed $\frac{RS22}{\sin\beta}$. The case of a strut passing through the axis can be done by using two separate struts that meet at the axis.

STRUT diameter should not exceed four wavelengths. Maximum number of struts is 4. Beta should be in the range 0° to 90° .

For best results, strut angle BETA should be large enough so that sampling points are less than a $1/4$ wavelength apart, i.e., $\sin \beta > \frac{2D/\lambda}{NAP}$.

FEED PATTERN

The maximum number of points to fit the pattern (N2) is 50.

REFLECTOR

Maximum diameter is 100 wavelengths.

INPUT FORMAT

GENERAL COMMENTS

All distance parameters required for input are in inches; all angles should be specified in degrees.

All decimal numbers may be anywhere within their specified field; all integers must be right adjusted. The decimal point must explicitly appear for all decimal numbers.

Comments may be typed on any card to the right of specified fields.

REFLECTOR GEOMETRY CARD

PURPOSE: To enter geometry of reflector

CARD:

	10	20	30	35
D2		FREQ	FDR	NAP

The numbers along the top refer to the last column in each field.

PARAMETERS: (I integer, F decimal number)

D2 (F) -diameter of reflector

FREQ (F)- frequency in MHZ

FDR (F) - ratio of focal distance f to diameter D

NAP (I) - number of aperture integration points.
If this parameter is less than 50,
or if it is omitted, 50 will be used.
If over 99 is used, 99 will be used.

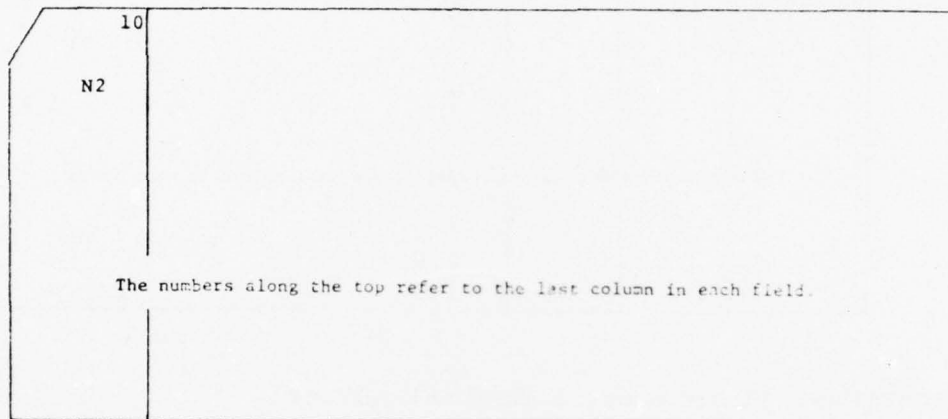
NOTES:

- The NAP parameter allows an increase of integration points over both the aperture and the strut for large sized reflectors, while allowing a smaller number of points and smaller computer costs for smaller problems. The value 99 may always be used if the computer cost is not objectionable.

FEED PATTERN CARD

PURPOSE: To provide data on number of points used to model primary feed pattern.

CARD:



PARAMETERS: (I integer, F decimal number)

N2 (I) - number of data points used to determine pattern in piecewise linear function.

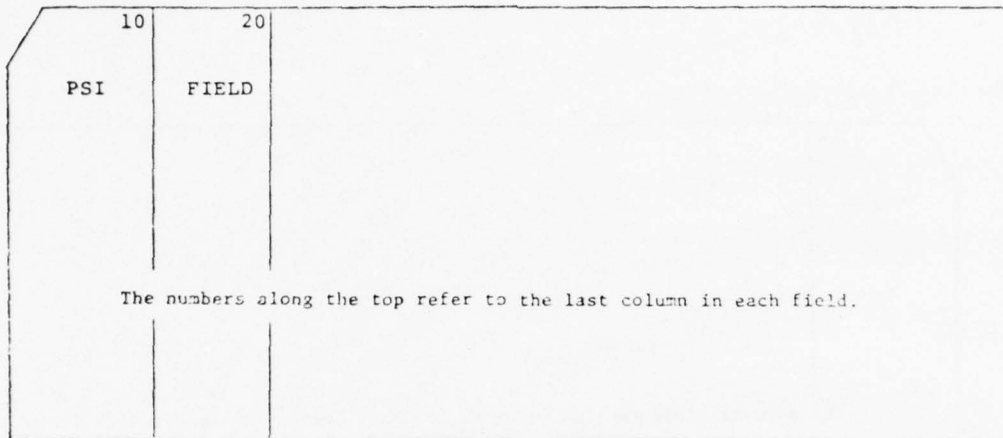
NOTES:

- This card determines how many cards of the next format will be read.

FEED PATTERN DATA CARDS

PURPOSE: To provide tabulated values of primary pattern.

CARD:



PARAMETERS: (I integer, F decimal number)

PSI (F) : Angle from axis of horn (-z axis of reflector, see figure 2) where tabulated value of field is to be supplied.

FIELD (F) : Field value of horn at that PSI angle.

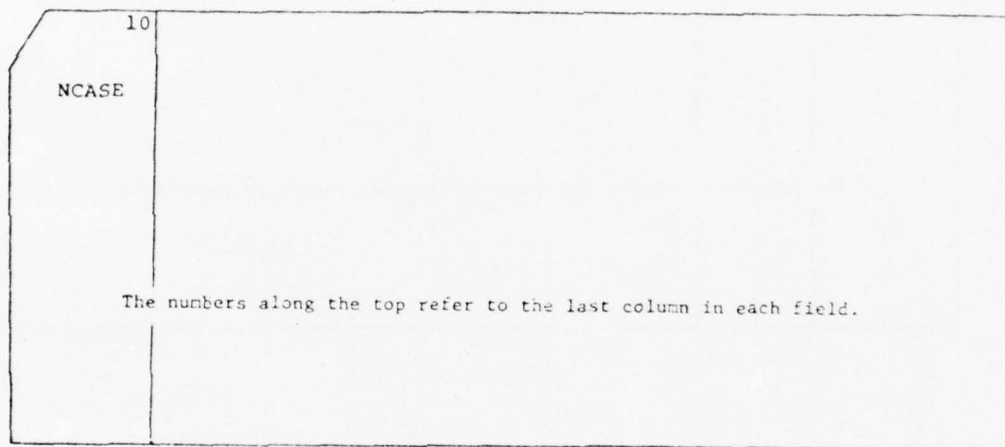
NOTES:

- There should be 2 groups of cards of this format.
N2 { Tabulated values to be interpolated by piece-
cards { wise linear function for E plane
- N2 { Tabulated values to be interpolated by piece-
cards { wise linear function for H plane
- For PSI larger than the last given value of PSI, a zero is assumed for the field value
- The maximum value of psi should subtend the edge of the reflector or erroneous results will occur.

NUMBER OF STRUT PROBLEMS CARD

PURPOSE: To indicate to the program how many problems will be done with the same reflector and feed pattern (above cards) but with different blockage parameters (below cards)

CARD:



PARAMETERS: (I integer, F decimal number)

NCASE (I) - number of different strut problems to be done with same reflector and feed pattern

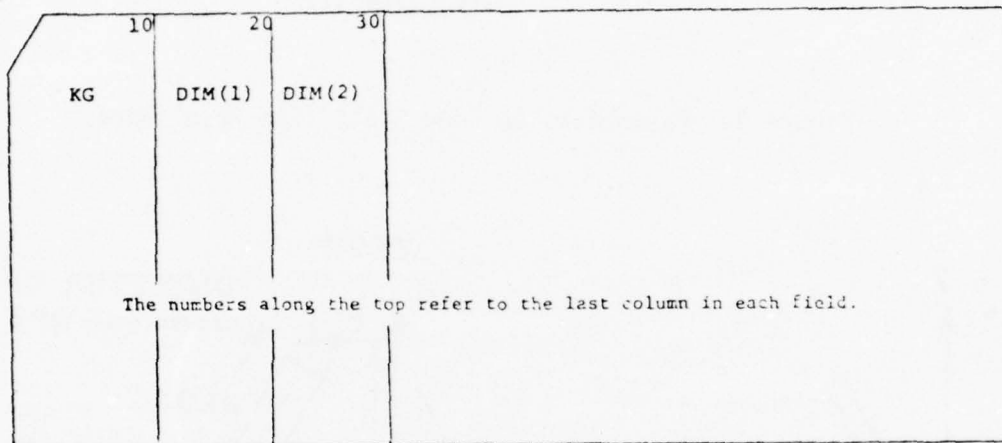
NOTES:

- If NCASE is not 1, the entire group of cards to be described below must be repeated NCASE times
- If the NCASE field is left blank, NCASE will be assigned 1. However, this card must always be present even if it is blank.

FEED SCATTERING MODEL CARD

PURPOSE: To describe size of feed aperture for blockage purposes.

CARD:



PARAMETERS: (I integer, F decimal number)

KG (I) - Code variable that indicates shape of feed aperture.

The values are: 1 - feed is circular
2 - feed is rectangular

DIM (1) (F) - These parameters are dimensions

DIM (2) (F) of feed (see figure 3)

If KG = 1, DIM (1) is radius

DIM (2) is ignored

If KG = 2, DIM (1) is length of feed in x direction

DIM (2) is length of feed in y direction

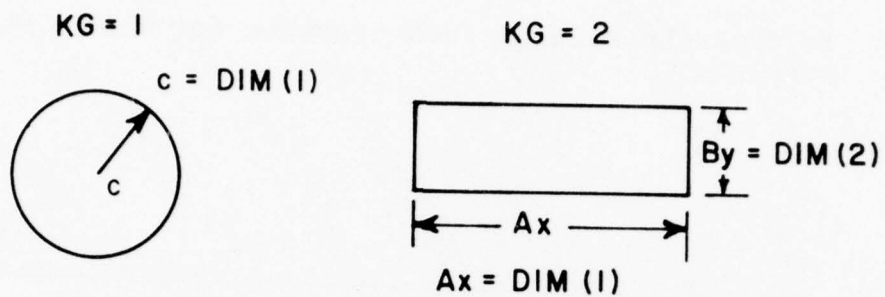


Figure 3. Parameters on Feed Scattering Model Card.

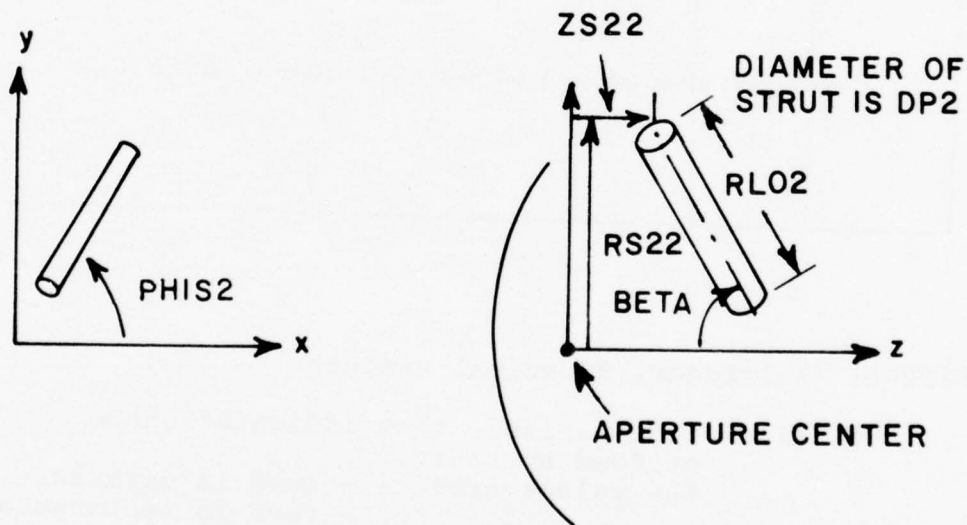
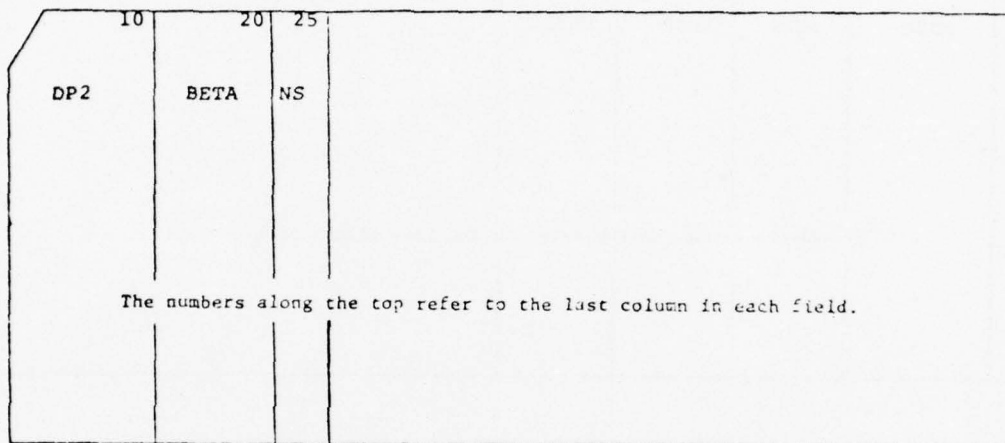


Figure 4. Strut Location Parameters.

COMMON STRUT DATA CARD

PURPOSE: To provide data that is common to all struts.

CARD:



PARAMETERS: (I integer, F decimal number)

DP2 (F) - diameter of struts

BETA (F) - angle of struts from -z axis
(see figure 4)

NS (I) - number of struts (cannot be more
than 4)

NOTES:

- This card causes NS cards of the next format to be read.

INDIVIDUAL STRUT DATA CARDS

PURPOSE: To describe data that may be different for each strut.

CARD:

10	20	30	40	
RS22	ZS22	RL02	PHIS2	
The numbers along the top refer to the last column in each field.				

PARAMETERS: (I integer, F decimal number)

- RS22 (F) - Radial distance of one end of the strut from z axis (see figure 4)
- ZS22 (F) - z coordinate of this same end
- RL02 (F) - length of strut
- PHIS2 (F) - ϕ (phi) angle of projection of strut in the xy plane

NOTES:

- For good accuracy there is a relationship between NAP, diameter of reflector in wave lengths, and angle BETA. For a given NAP, and diameter, the more nearly parallel the struts are to the z axis, the farther apart are integration points along the strut. This is the reason for the size restriction discussed under "limitations."
- Due to the analytical modeling done, any part of a strut whose projection falls outside the aperture will be ignored.
- There must be NS of these cards.

PHI CONTROL CARD

PURPOSE: To allow the user to specify which pattern cuts he wants.

CARD:

	10	20	30	40	50	60	70	80
NP		ANP (1)	ANP (2)	ANP (3)
The numbers along the top refer to the last column in each field.								

PARAMETERS: (I integer, F decimal number)

NP (I) - Absolute value is the number of phi cuts. If NP is positive, cuts will be evenly spaced. If NP is negative, cuts can be arbitrarily spaced.

ANP(1) (F) - Information on phi cuts: if evenly spaced case, ANP (1) is starting phi value and ANP (2) is increment between successive phi values. If arbitrary spaced case, the first NP values of ANP are the phi values.

NOTES:

- No comments are permitted on this one card since all possible fields are used.
- If arbitrary spaced phi's are used, limit is 7 different values. This limitation does not apply to evenly spaced cases.

THETA CONTROL CARD

PURPOSE: To set spacing and limits of field values within a phi cut.

CARD:

	10	20	30	
NTHETA		THONE	DTHETA	
The numbers along the top refer to the last column in each field.				

PARAMETERS: (I integer, F decimal number)

NTHETA (I) - number of theta values

THONE (F) - first theta value

DTHETA (F) - increment in theta values

NOTES:

- THONE should be assigned 0 to obtain proper normalization of secondary pattern.

PLOTTING CONTROL CARDS

A special group of cards, with a different mode of operation are used to control the plotting of data. This input, consisting of the AXIS, TITLE, CURVE, and NEXTPHI cards, can be rearranged to provide a wide variety of plotting options. Much of the data read in by these cards has an assumed default value. If the user does not provide some of this data, the program will assume a useful value. Hence, the user has the option of using standard size plots by entering only several numbers, or else, choosing his own plot format by entering additional data. Once the user has entered this data, it becomes the new assumed values for the rest of the program and this data does not need to be entered a second time unless it is desired to be changed.

AXIS CARD

PURPOSE: To cause the plotter to draw a new coordinate axis for the patterns to be subsequently plotted.

CARD:

	10	20	30	40	50	60	
AXIS	1	XLENGTH	YLENGTH	VLOW	VHI	PHILAB	
The numbers along the top refer to the last column in each field.							

PARAMETERS: (I integer, F decimal number)

- AXIS 1 : The word AXIS in columns 1 thru 4 and the number 1 in column 10 signifies which type of plotting card has been read.

- XLENGTH (F) : length of the horizontal axis (theta angle) in inches

- YLENGTH (F) : length of the vertical axis (field pattern) in inches

- VLOW (F) : value of the field pattern in db to labeled on lower point of vertical axis.

AXIS CARD (cont.)

VHI (F) : value of field pattern in db to
be labeled on highest point of
vertical axis.

PHILAB (F): decimal code that controls plotting
of the phi values. The values are:
1 = phi value for each individual
curve will be plotted. Use this
option when plotting different phi
cuts on the same axis.
0 = All the curves on a single axis
are for the same phi cut and phi
will be labeled only once for the
graph.

NOTES:

- The default values for this card are:

XLENGTH = 9.	VLOW = -72.
YLENGTH = 6.	VHI = 0.
PHILAB = 0.	

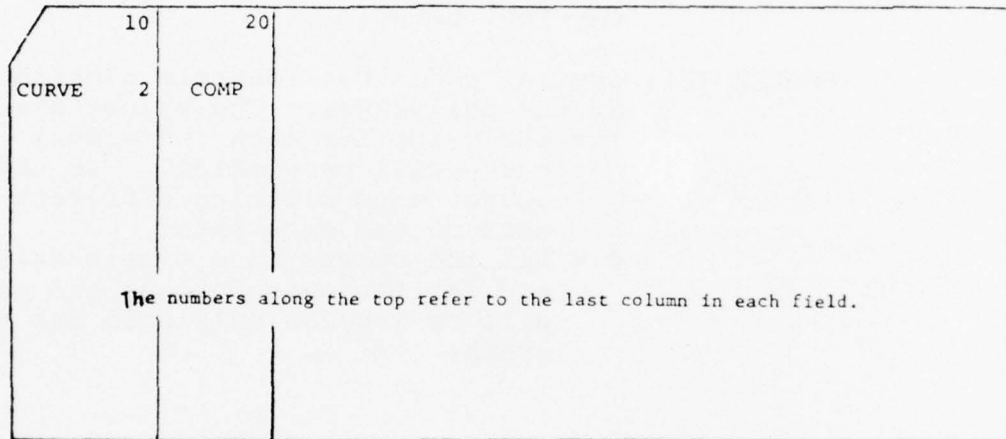
Thus the standard default plot has an axis 6" x 9"
with the 6" vertical scale ranging from 0 down to
-72 db. Only one phi cut angle label is provided.

- Labels on graphs make complete graph larger than just
dimension of coordinate system.

CURVE CARD

PURPOSE: To cause the computer to plot a selected component of the most recently computed phi cut and label it.

CARD:



PARAMETERS: (I integer, F decimal number)

CURVE 2 : The word CURVE in columns 1 thru 5 and the number 2 in column 10 signify which type of plotting card has been read.

COMP (I) : Component of field that is to be plotted. These component numbers are the same order as the magnitude in the output printout. The values are:
1 = for strut scattering, principal component
2 = for strut scattering, cross-polarized component
3 = for feed scattering, principal component
4 = for feed scattering, cross-polarized component
5 = for reflector + direct feed, principal component

CURVE CARD (cont.)

- 6 = for reflector + direct feed, cross-polarized component
- 7 = for total field, principal component
- 8 = for total field, cross-polarized component

NOTES:

- Any number of curves from the same phi cut can be plotted in the same graph by successive curve cards.
- Curves for strut scattering and feed scattering will be plotted only as far as $\theta \approx 90^\circ$ even if the maximum value of θ is larger. This is because these quantities are only calculated in this range. For $\theta > 90^\circ$, the reflector and direct feed and total fields are the same curves.
- Sections of curves that would go beneath the minimum plotted values VLOW specified on the AXIS card are drawn as straight lines at the bottom of the graph. This situation occurs for very deep nulls and for cross-polarized curves.

- AXIS card should precede the first CURVE card.

TITLE CARDS

PURPOSE: These two cards cause a user supplied title to be drawn beneath the coordinate axis.

CARD:

	10	20	
TITLE	4	NC	
The numbers along the top refer to the last column in each field.			

	80
text of title	
The numbers along the top refer to the last column in each field.	

PARAMETERS: (I integer, F decimal number)

TITLE 4 : The word TITLE in columns 1 thru
5 and the number 4 in column 10 signify
that this and the next card provide title
information.

NC (I) : The number of characters in the title
which will be given on 2nd card

SECOND card :
title: the first NC characters in this card
will appear centered beneath the
coordinate axis.

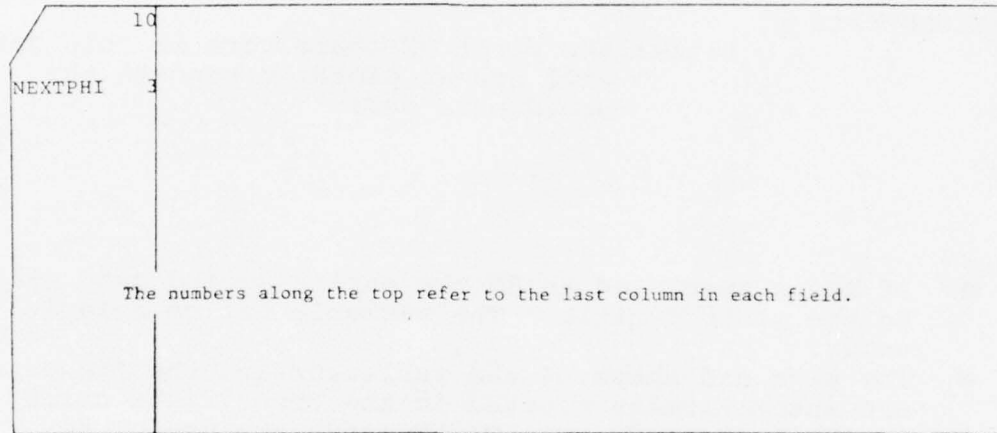
NOTES:

- If NC is specified as 80 the entire second card will be the plotted title. The variable has no default value.
- The size and shape of the reflector and the frequency are automatically plotted in the upper right corner by the AXIS card. The TITLE cards are useful to record the struts and feed details on the plot.

NEXTPHI CARD

PURPOSE: This card causes the next phi cut to be calculated after processing plot cards.

CARD:



PARAMETERS: (I integer, F decimal number)

NEXTPHI 3 : The word NEXTPHI in columns 1 thru 7 and the number 3 in column 10 signify what type of plot card this is. There are no other parameters on this card.

NEXTPHI CARD (cont.)

NOTES:

- This card is necessary to specify that the computer should calculate the next phi cut it has been previously given and not expect another plot command to plot a curve for the present phi cut.
- There should be as many NEXTPHI cards as there are phi cuts. Even if no plotting is desired the NEXTPHI card must appear. The program has been written so that if only NEXTPHI plot cards are used (no plotting is desired) then no calls to plot routines will be executed and no output plot file need be provided. The program is also written so that if plotting is never desired, only 1 card need be removed from the main program to eliminate reading NEXTPHI cards.
- After reading a NEXTPHI card, a new AXIS card needs to be read only if a new axis is desired. In this way, different phi cuts can be plotted on the same axis.

B. Example Computer Run

The input data for an example computer run are given in Table I. This example consists of three cases; the printed output data for the first case is given in Table II and the plotted output is given in Figures 5, 6 and 7. This example corresponds to a 24" diameter reflector with $F/D = 1/3$. For the first use there are three struts with diameter $2a_p = 0.37"$, $\beta = 68^\circ$ and $\phi_s = 90^\circ, 210^\circ, 330^\circ$, respectively. A circular flat plate with radius $c = 1.2"$ is used to model the feed. The pattern plane is $\phi = -15^\circ$ and the frequency is 11 GHz.

The printout of the first case, given in Table II, first echoes the input data, and then prints an interpolated input pattern that has been deduced from the arbitrarily spaced primary feed pattern data points. The printout of the coefficients of the scattered wave was used in the development of the program and can usually be ignored by the user. The bulk of the printout is the different contributions to the secondary field of the reflector. In the sample a theta spacing of $1/4^\circ$ was used so that the corresponding plot would have very smooth curves; a wider spacing can be used with increased roughness of plotted curves. The principal and cross-polarized components of each contribution are referenced to the Huygen polarization reference. After 90° , only the reflector and direct feed, and total fields are computed and listed. The printout for the rest of the three cases is similar and has been omitted.

Three examples of the computer plotting subroutines are shown in Figures 5, 6 and 7. The example in Figure 5 demonstrates the capability to plot the individual scattered field components: the basic contribution from the reflector and direct feed radiation, the strut scattering, the feed horn model scattering, and the total field which includes the various scattered field components. In this example only the principal polarization components are shown. The antenna geometry, pattern plane, and frequency correspond to the example computer run listed above. In this plot, the standard size and scale have been used.

The NEXTPHI 3 card causes more computations to be performed. Since only one value of phi has been specified above and since NCASE was read as 3 the next card is read as specifying a new strut and blockage problem with the same reflector geometry and primary feed. A new strut configuration with a single strut at $\phi = 90^\circ$ has been set. The second case, Figure 6 shows the capability to plot different pattern plane cuts: $\phi = -15^\circ, 0^\circ, 90^\circ$ are shown. In this example only the principally polarized component of the scattered field from

the struts are shown. Again the antenna geometry and frequency corresponds to the above computer run. Each NEXTPHI 3 card causes the phi values defined on the phi value card to be executed.

The capability to calculate cross-polarized components is shown in Figure 7 where only the total field is shown in both principal and cross polarizations. The reflector geometry, the direct feed pattern and the frequency are the same as above. However, instead of tripod struts, there is only one strut located at $\phi_s=20^\circ$. The strut diameter is 2.0 inches (1.86λ) and $\beta=68^\circ$. The strut length is the same as above. The strut angle $\phi_s=20^\circ$ and the large strut diameter was chosen to demonstrate a large cross polarized component of the strut scatter. This cross polarization effect dominates for $\phi>45^\circ$ in the $\phi=120^\circ$ plane which is near the scattering cone of the strut.

TABLE I - Input Data Card Listing

Card No.	Value	Category	
24.	11000.	Reflector Geometry Card Feed Pattern Card	
0.	1.		
10.	0.966		
20.	0.8714		
30.	0.7575		
40.	0.59		
50.	0.4522		
60.	0.336		
70.	0.2456		
80.	0.1813		
90.	0.15778		
120.	0.0917		
152.	0.079		
170.	0.02114		
180.	0.02427		
0.	1.		Feed Pattern Data Cards (E-plane)
10.	0.9575		
20.	0.6419		
30.	0.604		
40.	0.52		
50.	0.3772		
60.	0.2664		
70.	0.1866		
80.	0.1358		
90.	0.10521		
120.	0.05580		
152.	0.05475		
160.	0.01884		
180.	0.0224		
30.	0.353355	Feed Pattern Data Cards (H-plane)	

TABLE II
COMPUTER OUTPUT LISTING

CIRCULAR REFLECTOR ANTENNA FAR FIELD PATTERN WITH SCATTERING FROM FEED STRUTS AND FEED

ANTENNA GEOMETRY
APERTURE DIAMETER = 24.000 INCHES
 0.610 METERS
 22.352 WAVELLENGTH

LAMDA = 1.074
 0.027

FUCAL DISTANCE TO DIAMETER RATIO = 0.333

FREQUENCY = 11000.000 MHZ

NUMBER OF APERTURE POINTS = 50

NUMBER OF INPUT FEED VALUES = 14

PIECEWISE LINEAR FEED INPUT

PSI	F
0.0	1.00000
10.00	0.96600
20.00	0.91150
30.00	0.73750
40.00	0.59000
50.00	0.45200
60.00	0.32600
70.00	0.21500
80.00	0.13700
90.00	0.09100
100.00	0.07900
110.00	0.02114
120.00	0.02427

PIECEWISE LINEAR FEED INPUT

PSI	F
0.0	1.00000
10.00	0.97750
20.00	0.84190
30.00	0.68900
40.00	0.52000
50.00	0.37720
60.00	0.26640
70.00	0.18660
80.00	0.13580
90.00	0.10281
100.00	0.06475
110.00	0.01804
120.00	0.02240

BEST AVAILABLE COPY

BEST AVAILABLE COPY

FEED PATTERNS

PSI	FI	FEDS	FH	FHLH
0.0	1.0000	0.0	1.0000	0.0
5.00	0.9730	-0.1439	0.9730	-0.1866
10.00	0.9664	-0.3065	0.9575	-0.3772
15.00	0.9187	-0.7365	0.8997	-0.9160
20.00	0.8714	-1.1956	0.8419	-1.4968
25.00	0.8375	-1.6908	0.7830	-2.1501
30.00	0.8125	-2.2208	0.7240	-2.8969
35.00	0.7947	-2.7859	0.6650	-3.7401
40.00	0.7800	-3.3870	0.6060	-4.6828
45.00	0.7675	-4.0246	0.5470	-5.7298
50.00	0.7572	-4.6984	0.4880	-6.8866
55.00	0.7481	-5.4087	0.4290	-8.1483
60.00	0.7394	-6.1554	0.3700	-9.5199
65.00	0.7310	-6.9381	0.3110	-11.0000
70.00	0.7230	-7.7568	0.2520	-12.5881
75.00	0.7154	-8.6114	0.1930	-14.2827
80.00	0.7081	-9.5020	0.1340	-16.0822
85.00	0.7011	-10.4285	0.0750	-17.9859
90.00	0.6944	-11.3910	0.0160	-19.9934
95.00	0.6880	-12.3895	0.0570	-22.1042
100.00	0.6817	-13.4241	0.0980	-24.3284
105.00	0.6757	-14.4948	0.1390	-26.6662
110.00	0.6699	-15.6016	0.1800	-29.1179
115.00	0.6643	-16.7445	0.2210	-31.6832
120.00	0.6589	-17.9235	0.2620	-34.3622
125.00	0.6537	-19.1386	0.3030	-37.1547
130.00	0.6487	-20.3898	0.3440	-40.0607
135.00	0.6438	-21.6772	0.3850	-43.0802
140.00	0.6391	-23.0008	0.4260	-46.2132
145.00	0.6345	-24.3606	0.4670	-49.4607
150.00	0.6300	-25.7566	0.5080	-52.8227
155.00	0.6257	-27.1887	0.5490	-56.2992
160.00	0.6215	-28.6569	0.5900	-59.8902
165.00	0.6174	-30.1612	0.6310	-63.5957
170.00	0.6134	-31.7016	0.6720	-67.4167
175.00	0.6095	-33.2781	0.7130	-71.3532
180.00	0.6057	-34.8906	0.7540	-75.4052

FEED SCATTERING MODEL

CIRCULAR FEED BLOCKAGE

DIAMETER = 2.400
 INCHES
 0.061
 METERS
 2.235
 WAVELENGTH

FEED STRUTS

DIAMETER = 0.370 INCHES
 0.009 METERS
 0.345 WAVELENGTH

ETA = 68.0 DEGREES

NUMBER OF STRUTS = 3

STRUT NUMBER 1

PHI1 = 90.0 DEGREES

Z5

LENGTH
 INCHES
 METERS
 WAVELENGTH

RHO5
 10.800
 0.274
 10.028

-0.851
 -0.023
 -0.793

11.675
 0.296
 10.845

BEST AVAILABLE COPY

STRUT NUMBER 2	PHIS = 210.0 DEGREES	RHIS	Z S	LENGTH	INCHES METERS WAVELENGTH
		10.800	-0.051	11.645	
		0.274	-0.022	0.296	
		10.058	-0.093	10.845	

STRUT NUMBER 3	PHIS = 330.0 DEGREES	RHIS	Z S	LENGTH	INCHES METERS WAVELENGTH
		10.800	-0.051	11.645	
		0.274	-0.022	0.296	
		10.058	-0.093	10.845	

ARC = 1.0037

COEFFICIENTS OF THE SCATTERED WAVE FROM A CYLINDER

M	AH(M)	UH(M)
1	-0.793E+00	-0.122E+00
2	-0.243E+00	-0.123E+00
3	-0.494E-02	-0.710E-02
4	-0.118E-04	-0.121E-04
5	-0.587E-08	-0.610E-08
6	-0.990E-12	-0.733E-11
7	-0.723E-16	-0.769E-20
8	-0.263E-20	-0.554E-25
9	-0.646E-24	-0.687E-30
10	-0.547E-28	-0.541E-35
11	-0.287E-40	-0.288E-40
12		

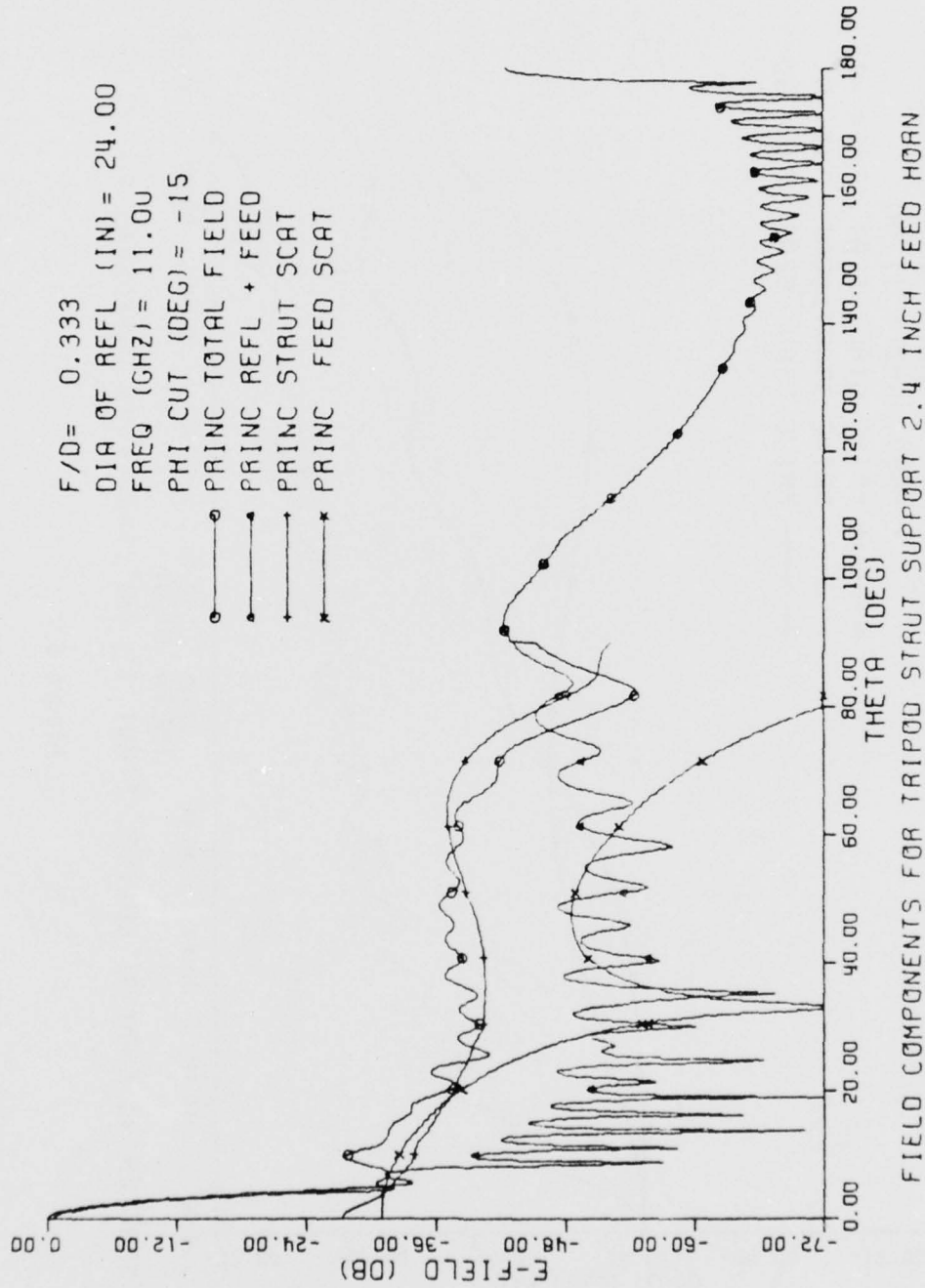


Figure 5.

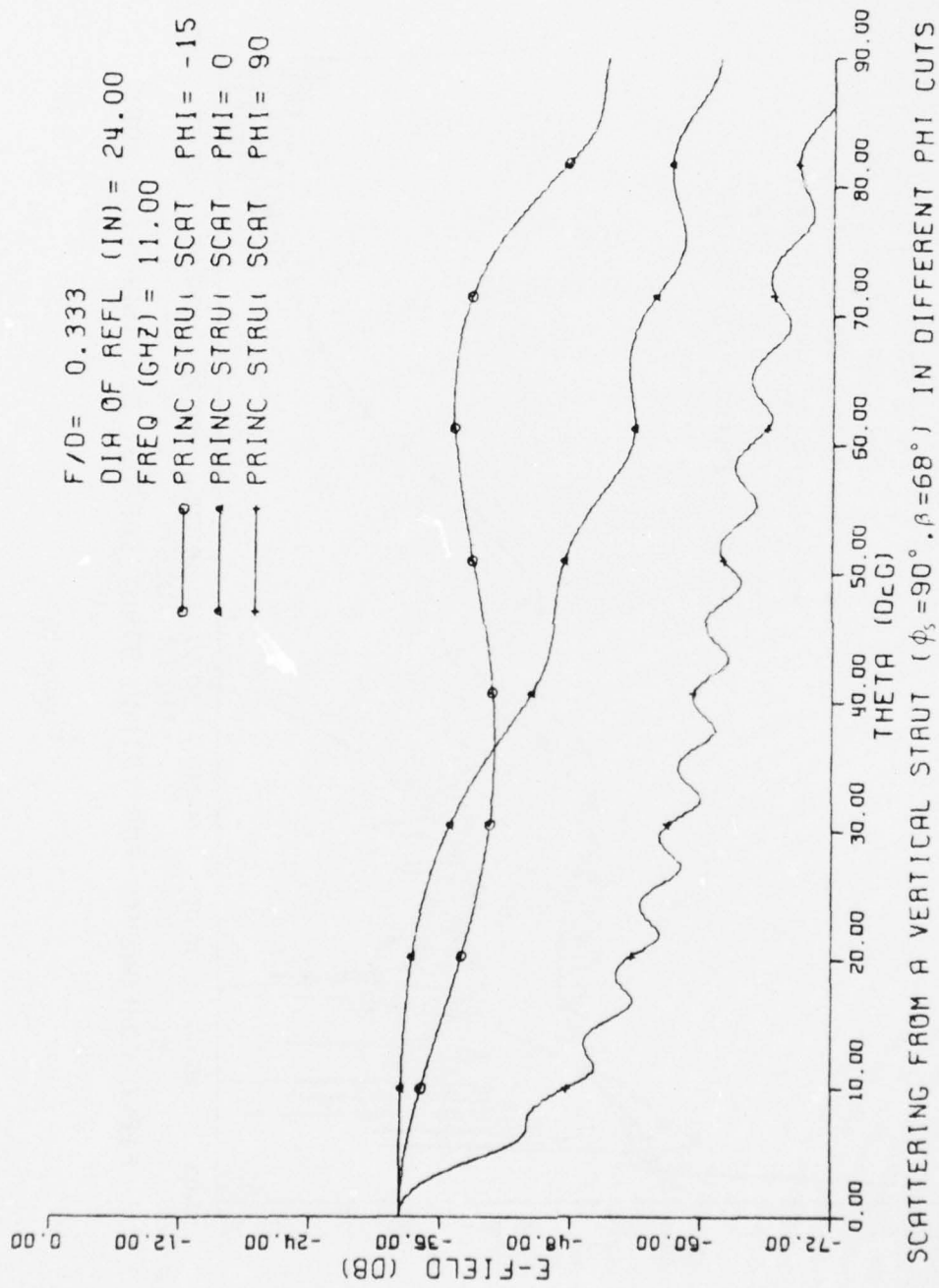


Figure 6.

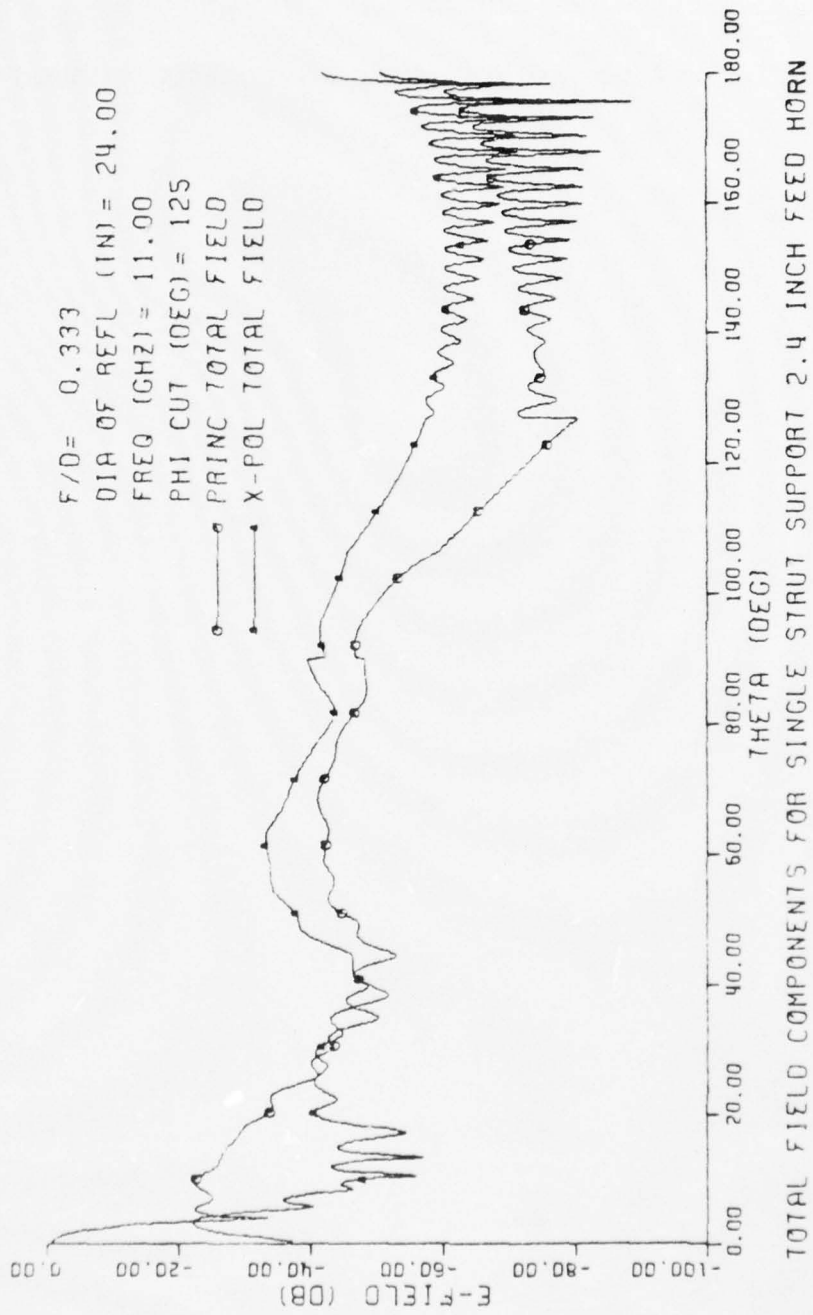


Figure 7.

C. Appendix - Computer Program Listing

The listing for the computer program described in this report is given below:

"Circular Reflector Antenna with Feed and Strut Scatter" (OSUPATT)


```

23 $T37,FR.3,T63,FR.3,TR0,* WAVELENGTH',//) OSU 1320
GO TO 25 OSU 1330
24 WRITE (6,24) DIM(1),DC1,DC OSU 1340
FORMAT (115,'CIRCULAR FEED BLOCKAGE',//T26,'DIAMETER =',FR.3,T55, OSU 1350
$' INCHES',/T36,FR.3,T55,' METERS',/T36,FR.3,T55,' WAVELENGTH',//) OSU 1360
CPP=2.*PI*C**2*C(XP(-J*RK*R))*CP OSU 1370
25 CONTINUE OSU 1380
C OSU 1390
C OSU 1400
C OSU 1410
C OSU 1420
C OSU 1430
READ (5,31) DP2,BETA,NS OSU 1440
31 FORMAT (2F10.5,15) OSU 1450
DP1=DP2*FM OSU 1460
OP=DP1/RLAM OSU 1470
AP=OP/2. OSU 1480
WRITE (6,32) DP2,BETA,NS,DP1,DP OSU 1490
32 FORMAT (110,'FEED STRUTS',//T24,'DIAMETER =',FR.3,' INCHES',T60, OSU 1500
$' BETA =',T6,1,' DEGREES',T90,'NUMBER OF STRUTS =',12,/T34,FR.3, OSU 1510
$' METERS',/T34,FR.3,' WAVELENGTH',//) OSU 1520
DO 35 I=1,NS OSU 1530
READ (5,33) RS22,ZS22,RL02,PHIS2 OSU 1540
33 FORMAT (4F10.5) OSU 1550
RS21=RS22*FM OSU 1560
ZS21=ZS22*FM OSU 1570
RL01=RL02*FM OSU 1580
RS2(I)=RS21/RLAM OSU 1590
ZS2(I)=ZS21/RLAM OSU 1600
RL0(I)=RL01/RLAM OSU 1610
WRITE (6,34) I,PHIS2,RS22,ZS22,RL02,RS21,ZS21,RL01,RS2(I), OSU 1620
$RL0(I) OSU 1630
34 FORMAT (T25,'STRUT NUMBER',12,//T50,'PHIS =',F5.1,' DEGREES',T80, OSU 1640
$'RHOS',T93,'ZS',T103,'LENGTH',//T73,3F12.3,T115,'INCHES',/T73, OSU 1650
$3F12.3,T115,' METERS',/T73,3F12.3,T115,' WAVELENGTH',//) OSU 1660
PHIS(I)=PHIS2*PI/180. OSU 1670
35 CONTINUE OSU 1680
C OSU 1690
C OSU 1700
C OSU 1710
C OSU 1720
C OSU 1730
BETN=BETA*PI/180. OSU 1740
SINB=SIN(BETN) OSU 1750
ARG=RK*AP*SINB OSU 1760
41 WRITE (6,41) ARG OSU 1770
FORMAT (//T10,'ARG=',FR.4,//) OSU 1780
MX=ARG+11 OSU 1790
DO 43 M=1,MX OSU 1800
L=M-1 OSU 1810
CALL BESJ(ARG,L,RSJ,0.001,IFR) OSU 1820
CALL BESY(ARG,L,RN,IFR) OSU 1830
BJ(M)=BSJ OSU 1840
HNK(M)=RSJ-J*RN OSU 1850
AM(M)=-BJ(M)/HNK(M) OSU 1860
IF (M.GT.1) GO TO 42 OSU 1870
AM(1)=0.5*AM(1) OSU 1880
GO TO 43 OSU 1890
42 BJP=BJ(L)-(L/ARG)*BJ(M) OSU 1900
HKP=HNK(L)-(L/ARG)*HNK(M) OSU 1910
BM(M)=-BJP/HKP OSU 1920
IF (ARG.GT.1.) GO TO 43 OSU 1930
PRA=REAL(AM(M))/REAL(AM(1)) OSU 1940
IF (PRA.GT.1.0E-8) GO TO 43 OSU 1950
RIA=AIMAG(AM(M))/AIMAG(AM(1)) OSU 1960
IF (RIA.GT.1.0E-8) GO TO 43 OSU 1970
GO TO 44 OSU 1980
43 CONTINUE OSU 1990

```

BEST AVAILABLE COPY


```

X=RK*A*SINT
IF (THETA.LT.90.) GO TO 67
IF (X.LT.2.5) GO TO 76
GO TO 70
IF (X.GT.24.) GO TO 70
62
C
C
C
C
C
*****
* APERTURE INTEGRATION *
*****
RHO=0.
DO 65 I=1,MI
XP=RK*RHO*SINT
IF (XP.GT.4.0E-2) GO TO 63
Y=(XP*XP)/4.
BJ0=1.-Y+Y*Y/4.
BJ2=Y/2.
BJ4=0.
GO TO 64
63 CALL BESJ(XP,0,BJ0,0.001,IFR1)
CALL BESJ(XP,2,BJ2,0.001,IFR1)
CALL BESJ(XP,4,BJ4,0.001,IFR1)
64 H(I)=-(SIN2P*TF(I)*BJ2+0.5*SIN4P*DF(I)*BJ4)*RHO*TM(I)/(2.*BET(I))
G(I)=-(TF(I)*BJ0+DF(I)*BJ2*COS2P)*RHO
RHO=RHO+DFL
65 CONTINUE
CALL QSF(DEL,H,ZX,MI)
CALL QSF(DEL,G,ZY,MI)
EX=CP*RK*COST*ZX(MI)
EY=CP*RK*COST*ZY(MI)
EZ=-CP*RK*SINT*(COSP*ZX(MI)+SINP*ZY(MI))
EP=-EX*SINP+EY*COSP
ET=FX*COST*COSP+EY*COST*SINP-EZ*SINT
IF (THETA.NE.0.0) GO TO 77
MAX=20.*ALOG10(CABS(EY))
WRITE (6,66) MAX
66 FORMAT (/15,'AXIAL FIELD =',F8.2,' DB',//)
GO TO 77
C
C
C
C
C
*****
* TWO POINT METHOD *
*****
70 T2=SQRT(A/SINT)
PS1=180.-THETA
S1=P1-THETA
SINS=SIN(S1)
COSS=COS(S1)
FAC=SQRT(1.-(SINS*SINP)**2)
IF (FAC.EQ.0.) GO TO 71
FT=COSS*SINP/FAC
FP=COSSP/FAC
GO TO 72
71 FT=1.
FP=0.
72 CP1=C*EXP(J*RK*(A*SINT-R0))
CP2=C*EXP(-J*RK*(A*SINT+R0))
PHI1=180.-GAMMA+THETA
PHI2=180.-GAMMA-THETA
IF (PHI2.LE.0.0) PHI2=360.+PHI2
CALL GTD(PHI1,PHIP,90.,S,RO,WA,SL,AS1,ILOP,DS1,DH1)
CALL GTD(PHI2,PHIP,90.,S,RO,WA,SL,AS1,ILOP,DS2,DH2)
ET1=-T2*CP1*DH1*RP*FTA
ET2=-J*T2*CP2*DH2*RP*FTA
EP1=T2*CP1*DS1*RP*FPA
EP2=J*T2*CP2*DS2*RP*FPA
C

```

```

05U 2680
05U 2690
05U 2700
05U 2710
05U 2720
05U 2730
05U 2740
05U 2750
05U 2760
05U 2770
05U 2780
05U 2790
05U 2800
05U 2810
05U 2820
05U 2830
05U 2840
05U 2850
05U 2860
05U 2870
05U 2880
05U 2890
05U 2900
05U 2910
05U 2920
05U 2930
05U 2940
05U 2950
05U 2960
05U 2970
05U 2980
05U 2990
05U 3000
05U 3010
05U 3020
05U 3030
05U 3040
05U 3050
05U 3060
05U 3070
05U 3080
05U 3090
05U 3100
05U 3110
05U 3120
05U 3130
05U 3140
05U 3150
05U 3160
05U 3170
05U 3180
05U 3190
05U 3200
05U 3210
05U 3220
05U 3230
05U 3240
05U 3250
05U 3260
05U 3270
05U 3280
05U 3290
05U 3300
05U 3310
05U 3320
05U 3330
05U 3340
05U 3350

```

C
C
C
C

* DIRECT FEED *

```

FF=0.
IF (THETA.GT.AN1) GO TO 74
CALL LSUM(PSI,PXE,FFE,DLE,N3,FE)
CALL LSUM(PSI,PXH,FFH,DLH,N3,FH)
FF=((FE+FH)/2.-COS2P*(FE-FH)/2.)*F*CP3
EFT=-FF*FT
EFP=EF*EP
IF (THETA.LE.90..OR.THETA.GT.AN2) GO TO 75
EP2=0.
ET2=0.
EP=EP1+EP2+EFP
ET=ET1+ET2+EFT
GO TO 77

```

74

75

C
C
C
C
76

* RING CURRENT METHOD *

```

CONTINUE
CALL BESJ(X,0,BJ0,0.002,IER)
CALL BESJ(X,2,BJ2,0.001,IER)
CALL BESJ(X,4,BJ4,0.001,IER)
DSC=DS*CONST
A1=TS*(DH-DSC)+DL*(DH+DSC)/2.
A2=-TS*(DH+DSC)-DL*(DH-DSC)
A3=DL*(DH+DSC)/2.
DHC=DH*CONST
B1=TS*(DS-DHC)-DL*(DS+DHC)/2.
B2=-TS*(DS+DHC)+DL*(DS-DHC)
B3=-DL*(DS+DHC)/2.
FPL=-CP4*(A1*BJ0+A2*BJ2+A3*BJ4)
HPL=CP4*(B1*BJ0+B2*BJ2+B3*BJ4)
EY=-FPL*SINP**2+HPL*CO5P**2
ET=-EY*SINP
EP=EY*CO5P
CONTINUE

```

77

C
C
C
C

* FEED BLOCKAGE SCATTERING *

```

IF (THETA.LE.90.) GO TO 80
FFBY=0.
ET1=ET
ETP=EP
GO TO 85
IF (KG.EQ.1) GO TO 81
XA=RK*AX*SINT*CO5P/2.
XB=RK*BY*SINT*SINP/2.
IF (XA.EQ.0.0) GA=1.
IF (XA.GT.0.0) GA=SIN(XA)/XA
IF (XB.EQ.0.0) GB=1.
IF (XB.GT.0.0) GB=SIN(XB)/XB
FFBY=CPP*CP3*GA*GB
GO TO 82
CONTINUE
XC=RK*C*SINT
CALL BESJ(XC,1,BJ1,0.001,IER1)
IF (XC.EQ.0.) FFBY=CPP*CP3/2.
IF (XC.GT.0.) FFBY=CPP*CP3*BJ1/XC
CONTINUE
FFFP=FFBY*CO5P
FFFT=FFBY*SINP

```

80

81

82

OSU 3360
OSU 3370
OSU 3380
OSU 3390
OSU 3400
OSU 3410
OSU 3420
OSU 3430
OSU 3440
OSU 3450
OSU 3460
OSU 3470
OSU 3480
OSU 3490
OSU 3500
OSU 3510
OSU 3520
OSU 3530
OSU 3540
OSU 3550
OSU 3560
OSU 3570
OSU 3580
OSU 3590
OSU 3600
OSU 3610
OSU 3620
OSU 3630
OSU 3640
OSU 3650
OSU 3660
OSU 3670
OSU 3680
OSU 3690
OSU 3700
OSU 3710
OSU 3720
OSU 3730
OSU 3740
OSU 3750
OSU 3760
OSU 3770
OSU 3780
OSU 3790
OSU 3800
OSU 3810
OSU 3820
OSU 3830
OSU 3840
OSU 3850
OSU 3860
OSU 3870
OSU 3880
OSU 3890
OSU 3900
OSU 3910
OSU 3920
OSU 3930
OSU 3940
OSU 3950
OSU 3960
OSU 3970
OSU 3980
OSU 3990
OSU 4000
OSU 4010
OSU 4020
OSU 4030


```

C   AXIS CASE
    IF (IFIRST .EQ. 0.) CALL PLOT ( XAXIS+3.,0.,-3)
    IF ( DATA(1) .NE. 0.) XAXIS=DATA(1)
    IF ( DATA(2) .NE. 0.) YAXIS=DATA(2)
    IF ( DATA(3) .NE. 0.) VL=DATA(3)
    IF ( DATA(4) .NE. 0.) VT=DATA(4)
    IF ( DATA(5) .NE. 0.) PC=1.
    IF ( DATA(5) .EQ. 0.) PC=0.
C   PC IS REAL CODE VARIABLE 1. IS INDIVIDUAL PHI LABELS
    DX=TMAX/XAXIS
    DY=(VT-VL)/YAXIS
    ICRV=0
    CALL AXIS(0.,0.,'THETA (DEG)',-11,XAXIS,0.,0.,DX,1.)
    CALL AXIS(0.,0.,'F-FIELD (DB)',12,YAXIS,90.,VL,DY,1.)
C   DRAW F/D, DIA AND FREQ LABELS
    XCOL=XAXIS-4.
    YCOL=YAXIS-.25
    XC=XCOL+.5.*CW
    CALL SYMBOL(XC,YCOL,HT,'F/D=',0.,4)
    CALL NUMBER(XC+.6.*CW,YCOL,HT,FOD,0.,3)
    YCOL=YCOL-VS
    CALL SYMBOL(XC,YCOL,HT,'DIA OF REFL (IN)=' ,0.,17)
    CALL NUMBER(XC+18.*CW,YCOL,HT,DIA,0.,2)
    YCOL=YCOL-VS
    CALL SYMBOL(XC,YCOL,HT,'FREQ (GHZ)=' ,0.,11)
    CALL NUMBER(XC+12.*CW,YCOL,HT,FREQ,0.,2)
    YCOL=YCOL-VS
    IF ( PC .EQ. 1.) GO TO 4
C   DRAW COMMON PHI LABEL
    CALL SYMBOL(XC,YCOL,HT,'PHI CUT (DEG)=' ,0.,14)
    CALL NUMBER(XC+15.*CW,YCOL,HT,PHI,0.,-1)
    YCOL=YCOL-VS
    GO TO 4
3  IF ( NTYPE .NE. 4) GO TO 6
C   PLOT TITLE
    NC=DATA(1)
    READ(5,7) ITITLE
7  FORMAT(20A4)
    XT=(XAXIS-NC)*CW/2.
    CALL SYMBOL(XT,-.75,HT,ITITLE(1),0.,NC)
    GO TO 4
6  IF ( NTYPE .NE. 2) GO TO 5
C   PLOT CURVE
    IF ( DATA(1) .NE. 0.) NCOM=DATA(1)
    ICRV=ICRV+1
    NP=NTHETA
    IF ( NCOM.LT. 5 .AND. TMAX .GT. 90.) NP=90./DT+1
    DDY=XAXIS/(NTHETA-1)
    IC=2
    DO 8 I=1,NP
    X=(I-1)*DDY
    Y=(PLOTST(NCOM,I)-VL)/DY
    IF ( Y .LT. 0.) Y=0.
    IF ( Y .GT. YAXIS) Y=YAXIS
    CALL PLOT(X,Y,IC)
    IF ((I/IX)*IX.EQ.1) CALL SYMBOL(X,Y,.07,ICRV,0.,-1)
8  IC=2
C   LABEL CURVE
    CALL SYMBOL(XC-1.,YCOL+HT/2.,.07,ICRV,0.,-1)
    CALL PLOT(XC-.2,YCOL+HT/2.,2)
    CALL SYMBOL(XC-.2,YCOL+HT/2.,.07,ICRV,0.,-1)
    CALL LABEL(XC,YCOL,HT,NCOM,'PRINC STRUT SCAT ',
1  'X-POL STRUT SCAT ', 'PRINC FEED SCAT ', 'X-POL FEED SCAT ',
2  'PRINC REFL + FEED', 'X-POL REFL + FEED', 'PRINC TOTAL FIELD',
6  'X-POL TOTAL FIELD')
    IF ( PC .EQ. 0.) GO TO 9
C   LABEL INDIVIDUAL PHI CUT
    CALL SYMBOL(XC+18.*CW,YCOL,HT,'PHI=' ,0.,4)

```

```

OSU 4720
OSU 4730
OSU 4740
OSU 4750
OSU 4760
OSU 4770
OSU 4780
OSU 4790
OSU 4800
OSU 4810
OSU 4820
OSU 4830
OSU 4840
OSU 4850
OSU 4860
OSU 4870
OSU 4880
OSU 4890
OSU 4900
OSU 4910
OSU 4920
OSU 4930
OSU 4940
OSU 4950
OSU 4960
OSU 4970
OSU 4980
OSU 4990
OSU 5000
OSU 5010
OSU 5020
OSU 5030
OSU 5040
OSU 5050
OSU 5060
OSU 5070
OSU 5080
OSU 5090
OSU 5100
OSU 5110
OSU 5120
OSU 5130
OSU 5140
OSU 5150
OSU 5160
OSU 5170
OSU 5180
OSU 5190
OSU 5200
OSU 5210
OSU 5220
OSU 5230
OSU 5240
OSU 5250
OSU 5260
OSU 5270
OSU 5280
OSU 5290
OSU 5300
OSU 5310
OSU 5320
OSU 5330
OSU 5340
OSU 5350
OSU 5360
OSU 5370
OSU 5380
OSU 5390

```

CALL NUMBER(XC+23,*CW,YCOL,HT,PHI,0.,-1)	05U 5400
9 YCOL=YCOL-VS	05U 5410
CALL PLOT2	05U 5420
4 IFRST=0	05U 5430
GO TO 5	05U 5440
END	05U 5450
SUBROUTINE LABEL(X,Y,H,N,C1,C2,C3,C4,C5,C6,C7,C8)	05U 5460
DIMENSION C1(1),C2(1),C3(1),C4(1),C5(1),C6(1),C7(1),C8(1)	05U 5470
GO TO (1,2,3,4,5,6,7,8),N	05U 5480
1 CALL SYMBOL(X,Y,H,C1(1),0.,17)	05U 5490
GO TO 9	05U 5500
2 CALL SYMBOL(X,Y,H,C2(1),0.,17)	05U 5510
GO TO 9	05U 5520
3 CALL SYMBOL(X,Y,H,C3(1),0.,17)	05U 5530
GO TO 9	05U 5540
4 CALL SYMBOL(X,Y,H,C4(1),0.,17)	05U 5550
GO TO 9	05U 5560
5 CALL SYMBOL(X,Y,H,C5(1),0.,17)	05U 5570
GO TO 9	05U 5580
6 CALL SYMBOL(X,Y,H,C6(1),0.,17)	05U 5590
GO TO 9	05U 5600
7 CALL SYMBOL(X,Y,H,C7(1),0.,17)	05U 5610
GO TO 9	05U 5620
8 CALL SYMBOL(X,Y,H,C8(1),0.,17)	05U 5630
9 RETURN	05U 5640
END	05U 5650
SUBROUTINE HUYSRC(ETHETA,EPHI,COSP,SINP)	05U 5660
ROUTINE CONVERT ETHETA,EPHI TO E HUYGEN PRINCIPAL AND CROSS	05U 5670
POLARIZED COMPONENTS	05U 5680
COMPLEX ETHETA,EPHI,STOR	05U 5690
STOR=COSP*ETHETA-SINP*EPHI	05U 5700
ETHETA=SINP*ETHETA+COSP*EPHI	05U 5710
EPHI=STOR	05U 5720
RETURN	05U 5730
END	05U 5740
SUBROUTINE STRUT(PHI,THETA,PHIS,Z2,RS2,RL0,EST,ESP)	05U 5750
05U 5760	
05U 5770	
05U 5780	
05U 5790	
05U 5800	
05U 5810	
05U 5820	
05U 5830	
05U 5840	
05U 5850	
05U 5860	
05U 5870	
05U 5880	
05U 5890	
05U 5900	
05U 5910	
05U 5920	
05U 5930	
05U 5940	
05U 5950	
05U 5960	
05U 5970	
05U 5980	
05U 5990	
05U 6000	
05U 6010	
05U 6020	
05U 6030	
05U 6040	
05U 6050	
05U 6060	
05U 6070	

```

SIND=SIN(PHID)
COXA=SINT*SINR*COXD-COST*COXA
ALP=ARCCOS(COXA)
SINA=SIN(ALP)
SSG=SINT*SIND
SCG=-SINT*COXR*COXD-COST*SINR
GAM=ATAN2(SSG,SCG)
SING=SIN(GAM)
COSG=COS(GAM)
ALPHA=ALP*180./PI
GAMMA=GAM*180./PI
DS={0.,0.}
DH={0.,0.}
DO 10 M=1,MX
COSM=COS((M-1)*(PI-GAM))
TERMS=2.*AM(M)*COSM
TERMH=2.*BM(M)*COSM
DS=DS+TERMS
DH=DH+TERMH
10 CONTINUE
DS=TEMP*DS
DH=TEMP*DH
CAB=COXA+COXB
RL=RL1
DO 12 J=1,N1
CQ=CEXP(J*RK*RL*CAH)
K=I+J-1
EI=-(TF(K)-DF(K)*COSPS)
SUMY=EI*CQ
RSY(I)=REAL(SUMY)
ASY(I)=AIMAG(SUMY)
RL=RL+DELS
12 CONTINUE
CALL QSF(DFLS,RSY,RZY,N1)
CALL QSF(DFLS,ASY,AZY,N1)
QYQ=RZY(N1)+J*AZY(N1)
CQ1=CEXP(J*RK*(R1+RL1)*CAR/2.)
CQ2=CEXP(J*RK*(R2+RL2)*CAR/2.)
FN1=-(RL1-K)*(TF(L1)+DF(L1-1))-DF(L1)+DF(L1-1))/2.
FN2=-(R2-RL2)*(TF(L2)-DF(L2))/2.
QY=QYQ+FN1*CQ1+FN2*CQ2
10 EALP=-CPS*DS*SINA*QY*SINPS*CPO
EGAM=CPS*DH*SINA*QY*(-COSPS)*CPO
FAT=-(COXA*COSG*COXB+SINA*SINB)*COST*COXD+COXA*SING*COST*SIND+SINT
*(COXA*COSG*SINB-SINA*COXB)
FAP=(SINA*SINB+COXA*COSG*COXR)*SIND+COXA*SING*COXD
FGT=SING*(COXB*COST*COXD-SINR*SINT)+COSG*COST*SIND
FGP=COSG*COXD-SING*COXR*SIND
EAT=EALP*FAT
EAP=EALP*FAP
FGP=EGAM*FGP
EGT=EGAM*FGT
EST=FAT+FGT
ESP=FAP+FGP
RETURN
END
SUBROUTINE LNFD(DSI,PX,FF,N)
DIMENSION DSI(50),PX(50),FF(50)
WRITE(6,2)
2 FORMAT(//T10,'PIECEWISE LINEAR FEED INPUT',//T18,'PSI',T31,'F',/)
DO 20 I=1,N
READ(5,10) PX(I),FF(I)
10 FORMAT(F10.2,F10.5)
15 FORMAT(T10,F10.2,F15.5)
WRITE(6,15) PX(I),FF(I)
IF(I.EQ.1) GO TO 20
DSI(I-1)=(FF(I)-FF(I-1))/(PX(I)-PX(I-1))
20 CONTINUE

```

```

OSU 6080
OSU 6090
OSU 6100
OSU 6110
OSU 6120
OSU 6130
OSU 6140
OSU 6150
OSU 6160
OSU 6170
OSU 6180
OSU 6190
OSU 6200
OSU 6210
OSU 6220
OSU 6230
OSU 6240
OSU 6250
OSU 6260
OSU 6270
OSU 6280
OSU 6290
OSU 6300
OSU 6310
OSU 6320
OSU 6330
OSU 6340
OSU 6350
OSU 6360
OSU 6370
OSU 6380
OSU 6390
OSU 6400
OSU 6410
OSU 6420
OSU 6430
OSU 6440
OSU 6450
OSU 6460
OSU 6470
OSU 6480
OSU 6490
OSU 6500
OSU 6510
OSU 6520
OSU 6530
OSU 6540
OSU 6550
OSU 6560
OSU 6570
OSU 6580
OSU 6590
OSU 6600
OSU 6610
OSU 6620
OSU 6630
OSU 6640
OSU 6650
OSU 6660
OSU 6670
OSU 6680
OSU 6690
OSU 6700
OSU 6710
OSU 6720
OSU 6730
OSU 6740
OSU 6750

```


	COMPLEX F,AJ,C0,C1,C2,C3,C4,DS,DH,FASE,0	OSU 7440
	REAL L,K1,K2	OSU 7450
	A(T,WN,N)=2.0*COS(3.14159265*WN*N-T/2.0)**2	OSU 7460
C	*** COMPUTE NECESSARY CONSTANTS	OSU 7470
C	PI=3.14159265	OSU 7480
C	PII=2.0*PI	OSU 7490
C	PI4=PI/4.0	OSU 7500
C	PI180=PI/180.	OSU 7510
C	AJ=CMPLX(0.,1.)	OSU 7520
C	EPSI=.0001	OSU 7530
C	W=50.	OSU 7540
C	GS=1.	OSU 7550
C	GH=1.	OSU 7560
C	WG=360.-WA	OSU 7570
C	IF (PHIP.EQ.0..OR.PHIP.EQ.WG) GS=0.	OSU 7580
C	IF (PHIP.EQ.0..OR.PHIP.EQ.WG) GH=.5	OSU 7590
C	*** COMPUTE ANGLES BETA-ZERO,BETA-POSITIVE,BETA-NEGATIVE	OSU 7600
C	WN=WG/180.	OSU 7610
C	BETAP=(PHI+PHIP)*PI180	OSU 7620
C	BETAN=(PHI-PHIP)*PI180	OSU 7630
C	*** CHOOSE DISTANCE PARAMETER FOR TYPE OF EGDE ILLUMINATION	OSU 7640
C	IF (ILOP.EQ.1) L=S*SIN(BETA0*PI180)**2	OSU 7650
C	IF (ILOP.EQ.2) L=S*SP/(S+SP)	OSU 7660
C	IF (ILOP.EQ.3) L=S*SP/(S+SP)*SIN(BETA0*PI180)**2	OSU 7670
C	IF (ILOP.EQ.4) L=SL	OSU 7680
C	*** COMPUTE A(S,SP) THE AMPLITUDE OF THE FIELD ALONG THE DIFFRACTED RA	OSU 7690
C	IF (ILOP.EQ.1) AS=1.0/SORT(S)	OSU 7700
C	IF (ILOP.EQ.2) AS=1.0/SORT(S*SIN(BETA0*PI180))	OSU 7710
C	IF (ILOP.EQ.3) AS=SORT(SP/(S*(S+SP)))	OSU 7720
C	IF (ILOP.EQ.4) AS=1.0	OSU 7730
C	*** COMPUTE ANGULAR ARGUMENTS FOR COTANGENT FUNCTION	OSU 7740
C	ANG1=(PI+BETAN)/(2.0*WN)	OSU 7750
C	ANG2=(PI-BETAN)/(2.0*WN)	OSU 7760
C	ANG3=(PI+BETAP)/(2.0*WN)	OSU 7770
C	ANG4=(PI-BETAP)/(2.0*WN)	OSU 7780
C	*** CALCULATE N+ AND N-	OSU 7790
C	NPN=IFIX((PI+BETAN)/(PII*WN)+0.5)	OSU 7800
C	NNN=IFIX((-PI+BETAN)/(PII*WN)+0.5)	OSU 7810
C	NPP=IFIX((PI+BETAP)/(PII*WN)+0.5)	OSU 7820
C	*** COMPUTE ARGUMENTS OF TRANSITION FUNCTION F(X) X=KLA	OSU 7830
C	ARG1=PII*L*A(BETAN,WN,NPN)	OSU 7840
C	ARG2=PII*L*A(BETAN,WN,NNN)	OSU 7850
C	ARG3=PII*L*A(BETAP,WN,NPP)	OSU 7860
C	ARG4=PII*L*A(BETAP,WN,NNP)	OSU 7870
C	*** DS AND DH CALCULATED BY KELLER'S FORM WHEN FIELD POINT IS NOT IN	OSU 7880
C	NNP=IFIX((-PI+BETAP)/(PII*WN)+0.5)	OSU 7890
C	TRANSITION REGIONS	OSU 7900
C	IF (ARG1.LE.W) GO TO 50	OSU 7910
C	IF (ARG2.LE.W) GO TO 50	OSU 7920
C	IF (ARG3.LE.W) GO TO 50	OSU 7930
C	IF (ARG4.LE.W) GO TO 50	OSU 7940
C	CO=SIN(PI/WN)*CEXP(-AJ*PI4)/(WN*PII*SIN(BETA0*PI180))	OSU 7950
		OSU 7960
		OSU 7970
		OSU 7980
		OSU 7990
		OSU 8000
		OSU 8010
		OSU 8020
		OSU 8030
		OSU 8040
		OSU 8050
		OSU 8060
		OSU 8070
		OSU 8080
		OSU 8090
		OSU 8100
		OSU 8110

AD-A043 400

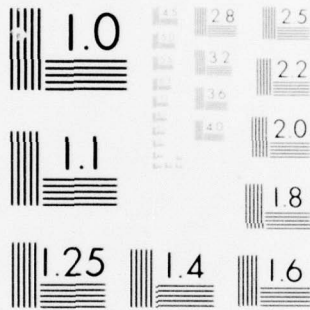
OHIO STATE UNIV COLUMBUS DEPT OF ELECTRICAL ENGINEERING F/G 9/1
A GTD ANALYSIS OF THE CIRCULAR REFLECTOR ANTENNA INCLUDING FEED--ETC(U)
AUG 77 S H LEE, R C RUDDUCK, C A KLEIN F30602-76-C-0224
4381-1 RADC-TR-77-259 NL

UNCLASSIFIED

2 OF 2
AD
A043400



END
DATE
FILMED
9 -77
DDC



MICROCOPY RESOLUTION TEST CHART
NATIONAL BUREAU OF STANDARDS-1963-A

C	MZERO=MAXO(MA,MB)	OSU10160
C	SET UPPER LIMIT OF M	OSU10170
C	MMAX=NTEST	OSU10180
100	DO 190 M=MZERO,MMAX,3	OSU10190
C	SET F(M),F(M-1)	OSU10200
C	FMI=1.0E-2H	OSU10210
	FM=.0	OSU10220
	ALPHA=.0	OSU10230
110	IF (M-(M/2)*2)120,110,120	OSU10240
	JT=-1	OSU10250
	GO TO 130	OSU10260
120	JT=1	OSU10270
130	M2=M-2	OSU10280
	DO 160 K=1,M2	OSU10290
	MK=M-K	OSU10300
	BMK=2.*FLOAT(MK)*FMI/X-FM	OSU10310
	FM=FM1	OSU10320
	FMI=BMK	OSU10330
140	IF (MK-N-1)150,140,150	OSU10340
	BJ=BMK	OSU10350
150	JT=-JT	OSU10360
	S=1+JT	OSU10370
160	ALPHA=ALPHA+BMK*S	OSU10380
	BMK=2.*FMI/X-FM	OSU10390
	IF (N)180,170,180	OSU10400
170	BJ=BMK	OSU10410
180	ALPHA=ALPHA+BMK	OSU10420
	BJ=BJ/ALPHA	OSU10430
190	IF (ABS(BJ-BPREV)-ABS(D*BJ))200,200,190	OSU10440
	BPREV=BJ	OSU10450
200	IFR=3	OSU10460
	RETURN	OSU10470
	END	OSU10480
	OSU10490
	SUBROUTINE BESY	OSU10500
	PURPOSE	OSU10510
	COMPUTE THE Y BESSEL FUNCTION FOR A GIVEN ARGUMENT AND ORDER	OSU10520
	USAGE	OSU10530
	CALL BESY(X,N,BY,IER)	OSU10540
	DESCRIPTION OF PARAMETERS	OSU10550
	X -THE ARGUMENT OF THE Y BESSEL FUNCTION DESIRED	OSU10560
	N -THE ORDER OF THE Y BESSEL FUNCTION DESIRED	OSU10570
	BY -THE RESULTANT Y BESSEL FUNCTION	OSU10580
	IER-RESULTANT ERROR CODE WHERE	OSU10590
	IER=0 NO ERROR	OSU10600
	IER=1 N IS NEGATIVE	OSU10610
	IER=2 X IS NEGATIVE OR ZERO	OSU10620
	IER=3 BY HAS EXCEEDED MAGNITUDE OF 10**70	OSU10630
	REMARKS	OSU10640
	VERY SMALL VALUES OF X MAY CAUSE THE RANGE OF THE LIBRARY	OSU10650
	FUNCTION ALOG TO BE EXCEEDD	OSU10660
	X MUST BE GREATER THAN ZERO	OSU10670
	N MUST BE GREATER THAN OR EQUAL TO ZERO	OSU10680
	SUBROUTINES AND FUNCTION SUBPROGRAMS REQUIRED	OSU10690
	NONE	OSU10700
	METHOD	OSU10710
		OSU10720
		OSU10730
		OSU10740
		OSU10750
		OSU10760
		OSU10770
		OSU10780
		OSU10790
		OSU10800
		OSU10810
		OSU10820
		OSU10830

C	CHECK IF ONLY Y0 OR Y1 IS DESIRED	OSU11520
C		OSU11530
C	90 IF(N-1)100,100,130	OSU11540
C		OSU11550
C	RETURN EITHER Y0 OR Y1 AS REQUIRED	OSU11560
C		OSU11570
C	100 IF(N)110,120,110	OSU11580
C	110 BY=Y1	OSU11590
C	GO TO 170	OSU11600
C	120 BY=Y0	OSU11610
C	GO TO 170	OSU11620
C		OSU11630
C	PERFORM RECURRENCE OPERATIONS TO FIND YN(X)	OSU11640
C		OSU11650
C	130 YA=Y0	OSU11660
C	YB=Y1	OSU11670
C	K=1	OSU11680
C	140 T=FLOAT(2*K)/X	OSU11690
C	YC=T*YB-YA	OSU11700
C	IF(ABS(YC)-1.0E70)145,145,141	OSU11710
C	141 IFR=3	OSU11720
C	RETURN	OSU11730
C	145 K=K+1	OSU11740
C	IF(K-N)150,160,150	OSU11750
C	150 YA=YB	OSU11760
C	YB=YC	OSU11770
C	GO TO 140	OSU11780
C	160 BY=YC	OSU11790
C	170 RETURN	OSU11800
C	180 IER=1	OSU11810
C	RETURN	OSU11820
C	190 IER=2	OSU11830
C	RETURN	OSU11840
C	END	OSU11850
C		OSU11860
C	OSU11870
C		OSU11880
C	SUBROUTINE QSF	OSU11890
C		OSU11900
C	PURPOSE	OSU11910
C	TO COMPUTE THE VECTOR OF INTEGRAL VALUES FOR A GIVEN	OSU11920
C	EQUIDISTANT TABLE OF FUNCTION VALUES.	OSU11930
C		OSU11940
C	USAGE	OSU11950
C	CALL QSF (H,Y,Z,NDIM)	OSU11960
C		OSU11970
C	DESCRIPTION OF PARAMETERS	OSU11980
C	H - THE INCREMENT OF ARGUMENT VALUES.	OSU11990
C	Y - THE INPUT VECTOR OF FUNCTION VALUES.	OSU12000
C	Z - THE RESULTING VECTOR OF INTEGRAL VALUES. Z MAY BE	OSU12010
C	IDENTICAL WITH Y.	OSU12020
C	NDIM - THE DIMENSION OF VECTORS Y AND Z.	OSU12030
C		OSU12040
C	REMARKS	OSU12050
C	NO ACTION IN CASE NDIM LESS THAN 3.	OSU12060
C		OSU12070
C	SUBROUTINES AND FUNCTION SUBPROGRAMS REQUIRED	OSU12080
C	NONE	OSU12090
C		OSU12100
C	METHOD	OSU12110
C	BEGINNING WITH Z(1)=0, EVALUATION OF VECTOR Z IS DONE BY	OSU12120
C	MEANS OF SIMPSONS RULE TOGETHER WITH NEWTONS 3/8 RULE OR A	OSU12130
C	COMBINATION OF THESE TWO RULES. TRUNCATION ERROR IS OF	OSU12140
C	ORDER H**5 (I.E. FOURTH ORDER METHOD). ONLY IN CASE NDIM=3	OSU12150
C	TRUNCATION ERROR OF Z(2) IS OF ORDER H**4.	OSU12160
C	FOR REFERENCE, SEE	OSU12170
C	(1) F.B.HILDEBRAND, INTRODUCTION TO NUMERICAL ANALYSIS.	OSU12180
C		OSU12190

C		MCGRAW-HILL, NEW YORK/TORONTO/LONDON, 1956, PP.71-76.	OSU12200
C		(2) R.ZURMUEHL, PRAKTISCHE MATHEMATIK FUER INGENIEURE UND	OSU12210
C		PHYSIKER, SPRINGER, BERLIN/GOETTINGEN/HEIDELBERG, 1963,	OSU12220
C		PP.214-221.	OSU12230
C		OSU12240
C		SUBROUTINE OSF(H,Y,Z,NDIM)	OSU12250
C			OSU12260
C			OSU12270
C			OSU12280
C			OSU12290
C			OSU12300
C			OSU12310
C			OSU12320
C			OSU12330
C			OSU12340
C			OSU12350
C			OSU12360
C			OSU12370
C			OSU12380
C			OSU12390
C			OSU12400
C			OSU12410
C			OSU12420
C			OSU12430
C			OSU12440
C			OSU12450
C			OSU12460
C			OSU12470
C			OSU12480
C			OSU12490
C			OSU12500
C			OSU12510
C			OSU12520
C			OSU12530
C			OSU12540
C			OSU12550
C			OSU12560
C			OSU12570
C			OSU12580
C			OSU12590
C			OSU12600
C			OSU12610
C			OSU12620
C			OSU12630
C			OSU12640
C			OSU12650
C			OSU12660
C			OSU12670
C			OSU12680
C			OSU12690
C			OSU12700
C			OSU12710
C			OSU12720
C			OSU12730
C			OSU12740
C			OSU12750
C			OSU12760
C			OSU12770
C			OSU12780
C			OSU12790
C			OSU12800
C			OSU12810
C			OSU12820
C			OSU12830
C			OSU12840
C			OSU12850
C			OSU12860
C			OSU12870

MISSION
of
Rome Air Development Center

RADC plans and conducts research, exploratory and advanced development programs in command, control, and communications (C³) activities, and in the C³ areas of information sciences and intelligence. The principal technical mission areas are communications, electromagnetic guidance and control, surveillance of ground and aerospace objects, intelligence data collection and handling, information system technology, ionospheric propagation, solid state sciences, microwave physics and electronic reliability, maintainability and compatibility.

